Organization TC1600 Bldg/Room REMSEN

United States Patent and Trademark Office
P.O. Box 1450
Alexandria, VA 22313-1450
If Undeliverable Return in Ten Days

OFFICIAL BUSINESS
PENALTY FOR PRIVATE USE, $300

ADDRESSEE UNKNOWN

U.S. OFFICIAL MAIL
PENALTY FOR PRIVATE USE $300
PITNEY BOWES
02 1A $ 01.59⁰
0004204479 AUG 23 2006
MAILED FROM ZIP CODE 22314

AN EQUAL OPPORTUNITY EMPLOYER

USPTO MAIL CENTER
AUG 31 2006
RECEIVED

UNITED STATES PATENT AND TRADEMARK OFFICE

UNITED STATES DEPARTMENT OF COMMERCE
United States Patent and Trademark Office
Address: COMMISSIONER FOR PATENTS
P.O. Box 1450
Alexandria, Virginia 22313-1450
www.uspto.gov

APPLICATION NO.	FILING DATE	FIRST NAMED INVENTOR	ATTORNEY DOCKET NO.	CONFIRMATION NO.
10/609,346	06/26/2003	Zailin Yu	ZYU-0603	1103

7590 08/24/2006

FortuneRock Inc.
Attn: Dr. Zailin Yu
Apt. D109
3120 Saint Paul St.
Baltimore, MD 21218

EXAMINER	
MERTZ, PREMA MARIA	
ART UNIT	PAPER NUMBER
1646	

DATE MAILED: 08/24/2006

Please find below and/or attached an Office communication concerning this application or proceeding.

To:
Our parents, who encouraged us,
Our teachers, who enabled us, and
Our children, who put up with us.

Cover Art: One of a series of color studies of horse heart cytochrome c designed to show the influence of amino acid side chains on the protein's three-dimensional folding pattern. We have selected this study to symbolize the discipline of biochemistry: Both are beautiful but still in process and hence have numerous "rough edges." Drawing by Irving Geis in collaboration with Richard E. Dickerson.

Cover and part opening illustrations copyrighted by Irving Geis.

Cover Designer: Madelyn Lesure

Photo Research: John Schultz, Eloise Marion

Photo Research Manager: Stella Kupferberg

Illustration Coordinator: Edward Starr

Copy Editor: Jeannette Stiefel

Production Manager: Lucille Buonocore

Senior Production Supervisor: Linda Muriello

BIOCHEMISTRY
DONALD VOET
JUDITH G. VOET

Library of Congress Cataloging in Publication Data:

Voet, Donald.
Biochemistry / by Donald Voet and Judith G. Voet.
p. cm.
Includes bibliographical references.
ISBN 0-471-61769-5
1. Biochemistry. I. Voet, Judith G. II. Title.
QP514.2.V64 1990 89-16727
574.19'2—dc20 CIP

Printed in the United States of America

10 9 8 7 6 5 4 3 2

3. CHEMICAL EVOLUTION

Individuals, as well as whole species, are characterized by their inherited genetic compositions. An organism's genetic complement, as we shall see in Part V, specifies the amino acid sequences of all of its proteins together with their quantity and schedule of appearance in each cell. An organism's protein composition is therefore the direct expression of its genetic composition.

In this section, we concentrate on the evolutionary aspects of amino acid sequences, the study of the chemical evolution of proteins. Evolutionary changes, which stem from random mutational events, often alter a protein's primary structure. A mutational change in a protein, if it is to be propagated, must somehow increase, or at least not decrease, the probability that its owner will survive to reproduce. Many mutations are deleterious and often lethal in their effects and therefore rapidly die out. On rare occasions, however, a mutation arises that, as we shall see below, improves the fitness of its host in its natural environment.

A. Sickle-Cell Anemia: The Influence of Natural Selection

Hemoglobin, the red blood pigment, is a protein whose major function is to transport oxygen throughout the body. A molecule of hemoglobin is an $\alpha_2\beta_2$ tetramer; that is, it consists of two identical α chains and two identical β chains (Fig. 6-1d). Hemoglobin is contained in the erythrocytes (red blood cells; Greek *erythros*, red + *kytos*, a hollow vessel) of which it forms ~33% by weight in normal individuals. In every cycle of their voyage through the circulatory system, the erythrocytes, which are normally flexible biconcave discs (Fig. 6-1a), must squeeze through capillary blood vessels smaller in diameter than they are.

In individuals with [illegible] sickle-cell anemia, many erythrocytes assume an irregular crescentlike shape under conditions of low oxygen concentration typical of the capillaries (Fig. 6-11b). This "sickling" increases the erythrocytes' rigidity, which hinders their free passage through the capillaries. The sickled cells therefore impede the flow of blood in the capillaries such that, in a sickle-cell "crisis," the blood flow in some areas may be completely blocked, thereby giving rise to extensive tissue damage and excruciating pain. Moreover, individuals with sickle-cell anemia suffer from severe hemolytic anemia (a condition characterized by red cell destruction) because the increased mechanical fragility of their erythrocytes halves the normal 120-day lifetime of these cells. The debilitating effects of this disease are such that, before the latter half of this century, individuals with sickle-cell anemia rarely survived to maturity (although modern treatments by no means constitute a cure).

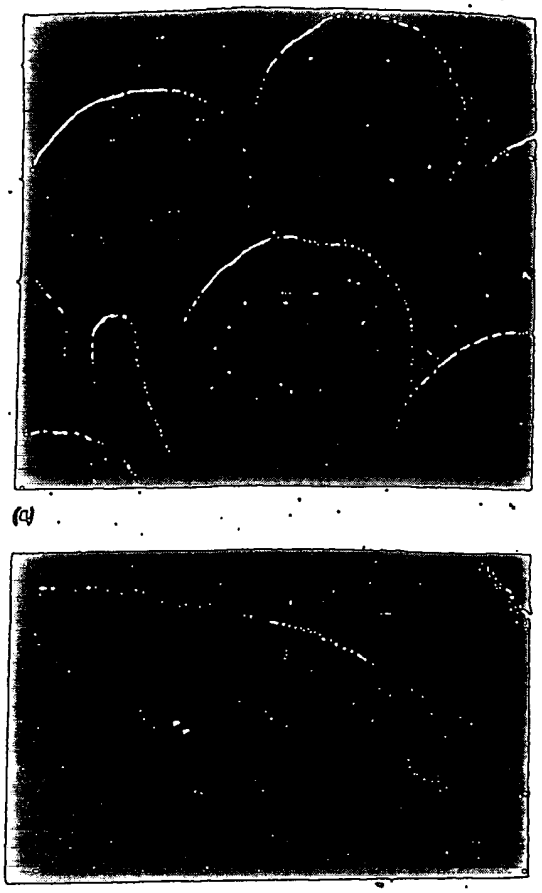

(a)

(b)

Figure 6-11
Scanning electron micrographs of: (a) Normal human erythrocytes revealing their biconcave disklike shape. [Dennis M. Prager/Visuals Unlimited.] (b) Sickled erythrocytes from patient with sickle-cell anemia. [© Langone/Photo Researchers, Inc.]

Sickle-Cell Anemia Is a Molecular Disease

In 1945, Linus Pauling correctly hypothesized that sickle-cell anemia, which he termed a *molecular disease*, is a result of the presence of a mutant hemoglobin. Pauling and his coworkers subsequently demonstrated, through electrophoretic studies, that normal human hemoglobin (HbA) has an anionic charge that is one and two units more negative than that of sickle-cell hemoglobin (HbS; Fig. 6-12).

In 1956, Vernon Ingram developed the technique of peptide mapping in order to pinpoint the difference between HbA and HbS. Ingram's fingerprints of tryptic digests of HbA and HbS revealed that their α subunits are identical but that their β subunits differ by a substitution in one tryptic peptide (Fig. 6-10). Sequencing studies indicated that this difference arises from the replacement of the Glu β6 of HbA (the Glu in the sixth position of each β chain) with Val in HbS (Glu β6 → Val). It

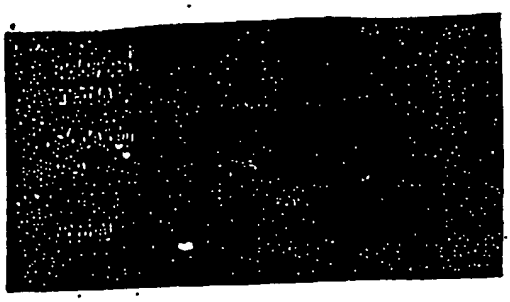

Figure 6-12
The electrophoretic pattern of hemoglobins from normal individuals and those with the sickle-cell trait and sickle-cell anemia. [From Montgomery, R., Dryer, R. L., Conway, T. W., and Spector, A. A., *Biochemistry, A Case Oriented Approach* (4th ed.), p. 67. Copyright © 1983 C. V. Mosby Company, Inc.]

accounting for the charge difference observed by Pauling. This was the first time an inherited disease was shown to arise from a specific amino acid change in a protein. *This mutation causes HbS to aggregate into filaments of sufficient size and stiffness to deform erythrocytes* —a remarkable example of the influence of primary structure on quaternary structure. The structure of these filaments is further discussed in Section 9-3B.

The Sickle-Cell Trait Confers Resistance to Malaria

Sickle-cell anemia is inherited according to the laws of Mendelian genetics (Section 27-1B). The cells of all higher organisms but germ cells have two homologous copies of each chromosome with the exception of sex chromosomes. An organism carrying a particular gene is classified as heterozygous or homozygous for that gene if its cells, respectively, bear one or two copies of that gene. The hemoglobin of individuals who are homozygous for sickle-cell anemia is almost entirely HbS. In contrast, individuals heterozygous for sickle-cell anemia have hemoglobin that is ~40% HbS (Fig. 6-12). Such persons, who are said to have the sickle-cell trait, lead a normal life even though their erythrocytes have a shorter lifetime than those of normal individuals.

The sickle-cell trait and disease occur mainly in persons of equatorial African descent. The regions of equatorial Africa where malaria is a major cause of death (contributing to childhood mortality rates as high as 50%), as Fig. 6-13 indicates, coincide closely with those areas where the sickle-cell gene is prevalent (possessed by as much as 40% of the population in some places). This observation led Anthony Allison to the discovery that *individuals heterozygous for HbS are resistant to malaria.*

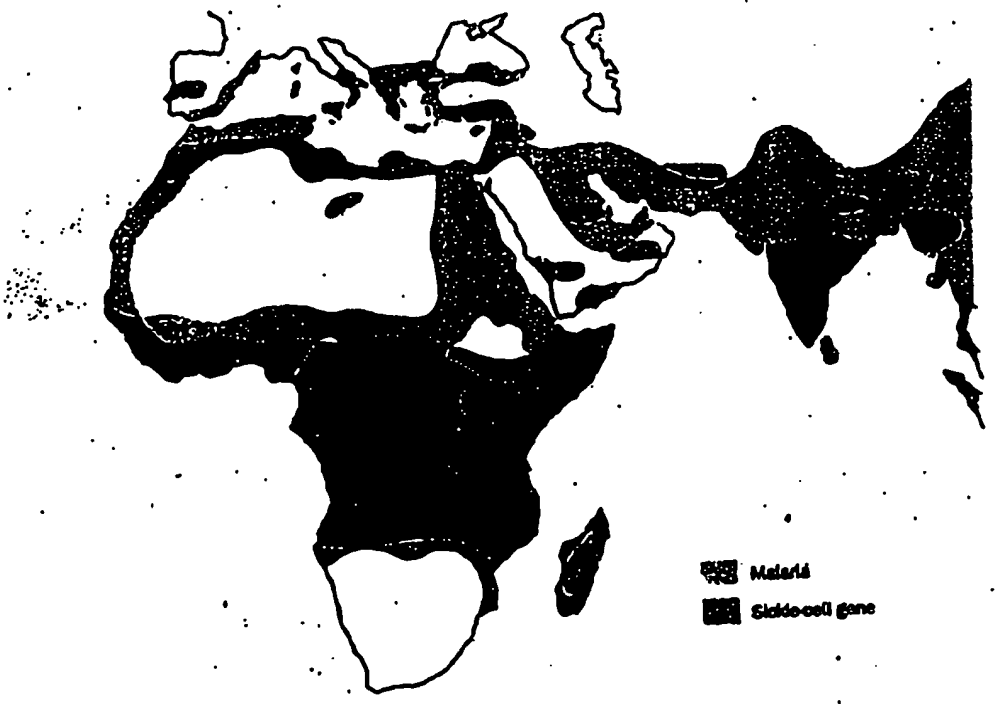

Figure 6-13
A map indicating the regions of the world where malaria caused by *P. falciparum* was prevalent before 1930, together with the distribution of the sickle-cell gene.

Table 6-4
Amino Acid Sequences of Cytochromes c from 38 Species[a]

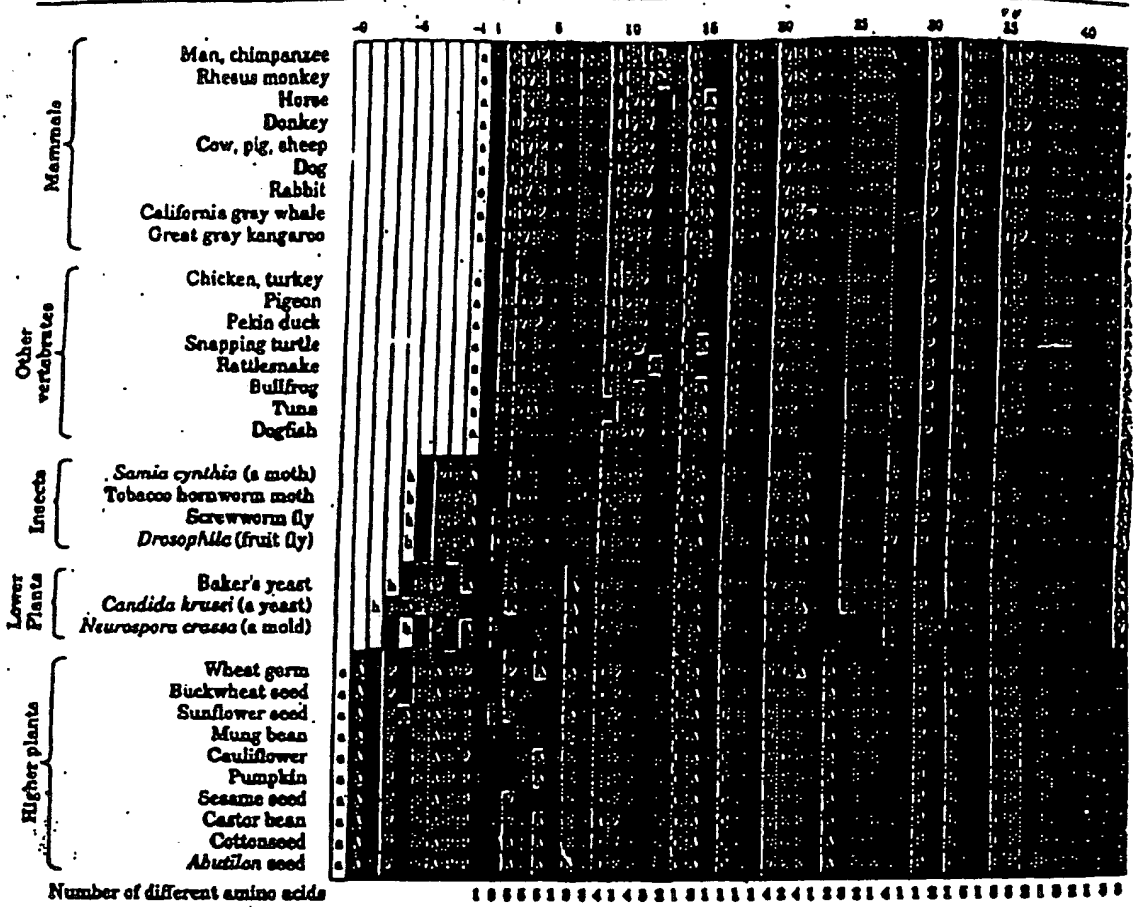

[a] The amino acid side chains have been shaded according to their polarity characteristics so that an invariant or conservatively substituted residue is identified by a vertical band of a single color. The letter a at the beginning of the chain indicates that the N-terminal amino group is acetylated; an h indicates the acetyl group is absent.

Source: After Dickerson, R. E., *Sci. Am.* 226(4): 58–72 (1972) with corrections from Dickerson, R. E., and Timkovich, R., *in* Boyer, P. D. (Ed.), *The Enzymes* (3rd ed.), Vol. 11, *pp.* 421–422, Academic Press (1975). Table copyrighted © by Irving Geis.

Malaria is a parasitic disease. In Africa it is caused by the mosquito-borne protozoan *Plasmodium falciparum*, which resides within an erythrocyte during much of its 48-h life cycle. *Plasmodia* increase the acidity of the erythrocytes they infect by −0.4 pH units and cause them to adhere to a specific protein lining blood vessel walls by protein knobs that develop on the erythrocyte surfaces (the spleen would otherwise remove the infected erythrocytes from the circulation thereby killing the parasites). Death often results when so many erythrocytes are lodged in a vital organ (such as the brain in cerebral malaria) that its blood flow is significantly impeded.

How does the sickle-cell trait confer malarial resistance? Normally, ~2% of the erythrocytes of individuals with the sickle-cell trait are observed to sickle under the low oxygen concentration conditions found in the capillaries. However, the lowered pH of infected erythrocytes increases their proportion of sickling in the capillaries to ~40%. A normal erythrocyte maintains a high internal concentration of K^+ relative to that of the blood serum through processes discussed in Section 18-3A. When an erythrocyte sickles, the permeability of its cell membrane to K^+ increases so that the K^+ concentration in sickled cells is lower than in normal erythrocytes. The malarial parasite requires a high K^+ concentration and

Bohr effect by 10%. In normal deoxyHb, the imidazole ring of His 146β associates with the carboxylate of Asp 94β on the same subunit (Figs. 9-18*b* and 9-19) to form a salt bridge that is absent in the R state. Proton NMR measurements indicate that formation of this salt bridge increases the pK of the imidazole group from 7.1 to 8.0. This effect more than accounts for His 146β's share of the Bohr effect.

About 30 to 40% of the Bohr effect remains unaccounted for. It no doubt arises from small contributions of many of the residues whose environments are altered upon hemoglobin's R → T transition. A variety of evidence suggests that His 122α, His 143β, and Lys 82β are among these residues.

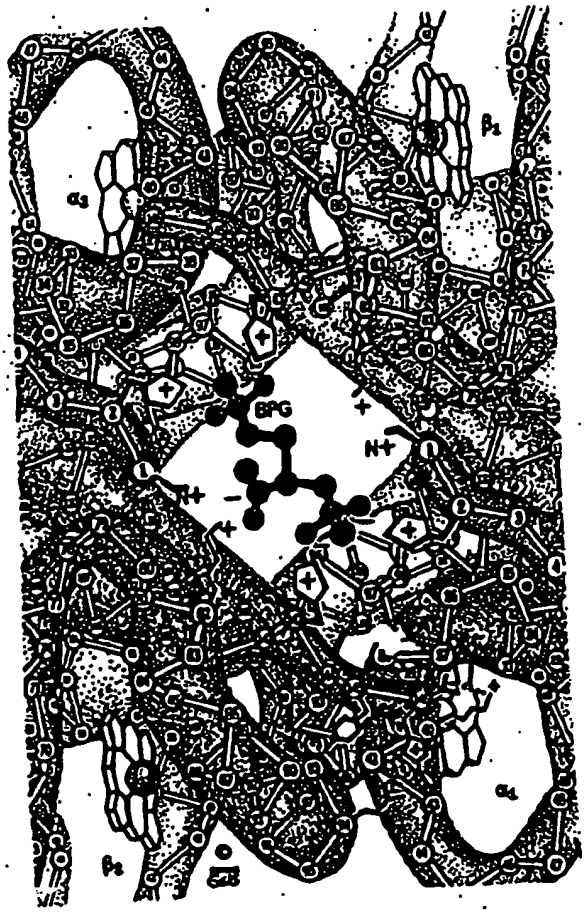

Figure 9-22
The binding of BPG to deoxyHb as viewed down the molecule's exact twofold axis (the same view as in Fig. 9-18*a*). BPG (red), with its five anionic groups, binds in the central cavity of deoxyHb where it is surrounded by a ring of eight cationic side chains (blue) extending from the two β subunits. In the R state, the central cavity is too narrow to contain BPG (Fig. 9-18*b*). The arrangement of salt bridges and hydrogen bonds between the α_1 and β_2 subunits that partially stabilizes the T state (Figs. 9-18*b* and 9-19) is indicated on the lower right. [Figure copyrighted © by Irving Geis.]

F. Structural Basis of BPG Binding

BPG decreases the oxygen-binding affinity of Hb b preferentially binding to its deoxy state (Section 9-1D The binding of the physiologically quadruply charge BPG to deoxyHb is weakened by high salt concentr tions, which suggests that this association is ionic i character. This explanation is corroborated by the X-ra structure of a BPG–deoxyHb complex, which indicate that BPG binds in the central cavity of deoxyHb on it twofold axis (Fig. 9-22). The anionic groups of BPG ar within hydrogen bonding and salt bridging distances c the cationic Lys EF6(82), His H21(143), His NA2(2), an N-terminal amino groups of both β subunits (Fig. 9-22. The T → R transformation brings the two β H helice together, which narrows the central cavity (compar Fig. 9-13*a* and *b*) and expels the BPG. It also widens th distance between the β N-terminal amino groups fror 16 to 20 Å, which prevents their simultaneous hydro gen bonding with BPG's phosphate groups. BPG there fore stabilizes the T conformation of Hb by cross-linkin its β subunits. This shifts the T ⇌ R equilibrium toward the T state, which lowers hemoglobin's O_2 affinity.

The structure of the BPG–deoxyHb complex also in dicates why fetal hemoglobin (HbF) has a reduced af finity for BPG relative to HbA (Section 9-1D). The cat ionic His H21(143)β of HbA is changed to an uncharge Ser residue in HbF's β-like γ subunit thereby eliminatin a pair of ionic interactions stabilizing the BPG deoxyHb complex (Fig. 9-22).

3. ABNORMAL HEMOGLOBINS

Mutant hemoglobins have provided a unique oppor tunity to study structure–function relationships in pro teins because Hb is the only protein of known structu that has a large number of well-characterized variant The examination of individuals with physiological di abilities together with the routine electrophoret screening of human blood samples has led to the discov ery of over 400 mutant hemoglobins. Around 95% these variants result from single amino acid substit tions in a globin polypeptide chain. In this section, v consider the nature of these hemoglobinopathies. H moglobin diseases characterized by defective glob synthesis, the thalassemias, are the subject of Secti 33-2G.

A. Molecular Pathology of Hemoglobin

The physiological effect of an amino acid substituti on Hb can, in most cases, be understood in terms of molecular location:

1. Changes in surface residues
Changes of surface residues are usually innocuous cause most of these residues have no specific functio role (although sickle-cell Hb (HbS) is a glaring exc

tion to this generalization; Section 9-3B]. For example, HbE [Glu B8(26)$\beta \rightarrow$ Lys], the most common human Hb mutant after HbS (possessed by up to 10% of the populace in parts of Southeast Asia), has no clinical manifestations in either heterozygotes or homozygotes. About one half of the known Hb mutations are of this type and were only discovered accidentally or through surveys of large populations. It has been estimated that one individual in 800 has a variant hemoglobin.

2. Changes in internally located residues

Changing an internal residue often destabilizes the Hb molecule. The degradation products of these hemoglobins, particularly those of heme, form granular precipitates (known as Heinz bodies) that are hydrophobically adsorbed to the erythrocyte cell membrane. The membrane's permeability is thereby increased causing premature cell lysis. Carriers of unstable hemoglobins therefore suffer from hemolytic anemia of varying degrees of severity.

The structure of Hb is so delicately balanced that small structural changes may render it nonfunctional. This can occur through the weakening of the heme–globin association or as a consequence of other conformational changes. For instance, the heme group is easily dislodged from its closely fitting hydrophobic binding pocket. This occurs in Hb Hammersmith (Hb variants are often named after the locality of their discovery) in which Phe CD1(42)β, an invariant residue that wedges the heme into its pocket (see Figs. 9-12 and 9-15), is replaced by Ser. The resulting gap permits water to enter the heme pocket, which causes the hydrophobic heme to easily drop out. Similarly, in Hb Bristol, the substitution of Asp for Val E11(67)β, which partially occludes the O_2 pocket, places a polar group in contact with the heme. This weakens the binding of the heme to the protein, probably by facilitating the access of water to the subunit's otherwise hydrophobic interior.

Hb may also be destabilized by the disruption of elements of its 2°, 3°, and/or 4° structures. The instability of Hb Bibba results from the substitution of a helix-breaking Pro for Leu H19(136)α. Likewise, the instability of Hb Savannah is caused by the substitution of Val for the highly conserved Gly B6(24)β, which is located on the B helix where it crosses the E helix with insufficient clearance for side chains larger than an H atom (Fig. 9-13, and Fig. 9-11 where Gly B6 is residue 25). The α_1–β_1 contact, which does not significantly dissociate under physiological conditions, may do so upon structural alteration. This occurs in Hb Philly in which Tyr C1(35)α, which participates in the hydrogen bonded network that helps knit together the α_1–β_1 interface, is replaced by Phe.

3. Changes stabilizing methemoglobin

Changes at the O_2-binding site that stabilize the heme in the Fe(II) oxidation state eliminate the binding of O_2 to the defective subunits. Such methemoglobins are designated HbM and individuals carrying them are said to have methemoglobinemia. These individuals usually have bluish skin, a condition known as cyanosis, which results from the presence of deoxyHb in their arterial blood.

All known methemoglobins arise from substitutions that provide the Fe atom with an anionic oxygen atom ligand. In Hb Boston, the substitution of Tyr for His E7(58)α (the distal His) results in the formation of a 5-coordinate Fe(III) complex with the phenolate ion of the mutant Tyr E7 displacing the imidazole ring of His F8(87) as the apical ligand (Fig. 9-23*a*). In Hb Milwaukee, the γ-carboxyl group of the Glu that replaces Val E11(67)β forms an ion pair with a 5-coordinate Fe(III) complex (Fig. 9-23*b*). Both the phenolate and glutamate ions in these methemoglobins so stabilize the Fe(III) oxidation state that methemoglobin reductase is ineffective in converting them to the Fe(II) form.

Individuals with HbM are alarmingly cyanotic and have blood that is chocolate brown, even when their normal subunits are oxygenated. In northern Japan, this condition is named "black mouth" and has been known for centuries; it is caused by the presence of HbM Iwate [His F8(87)$\alpha \rightarrow$ Tyr]. Methemoglobins have Hill constants of ~1.2. This indicates a reduced cooperativity in comparison with HbA even though HbM, which can only bind two oxygen molecules, can have a maximum Hill constant of 2 (the unmutated chains remain functional). Surprisingly, heterozygotes with HbM, which have an average of one functional β subunit per Hb molecule, have no apparent physical disabilities. Evidently, the amount of O_2 released in their capillaries is within normal limits. Homozygotes of HbM, however, are unknown; this condition is, no doubt, lethal.

4. Changes at the α_1–β_2 contact

Changes at the α_1–β_2 contact often interfere with hemoglobin's quaternary structural changes. Most such hemoglobins have an increased O_2 affinity so that they release less than normal amounts of O_2 in the tissues. Individuals with such defects compensate for it by increasing the concentration of erythrocytes in their blood. This condition, which is named polycythemia, often gives them a ruddy complexion. Some amino acid substitutions at the α_1–β_2 interface instead result in a reduced O_2 affinity. Individuals carrying such hemoglobins are cyanotic.

Amino acid substitutions at the α_1–β_2 contact may change the relative stabilities of hemoglobin's R and T forms, thereby altering its O_2 affinity. For example, the replacement of Asp G1(99)β by His in Hb Yakima eliminates the hydrogen bond at the α_1–β_2 contact that stabilizes the T form of Hb (Fig. 9-17*a*). The interloping imidazole ring also acts as a wedge that

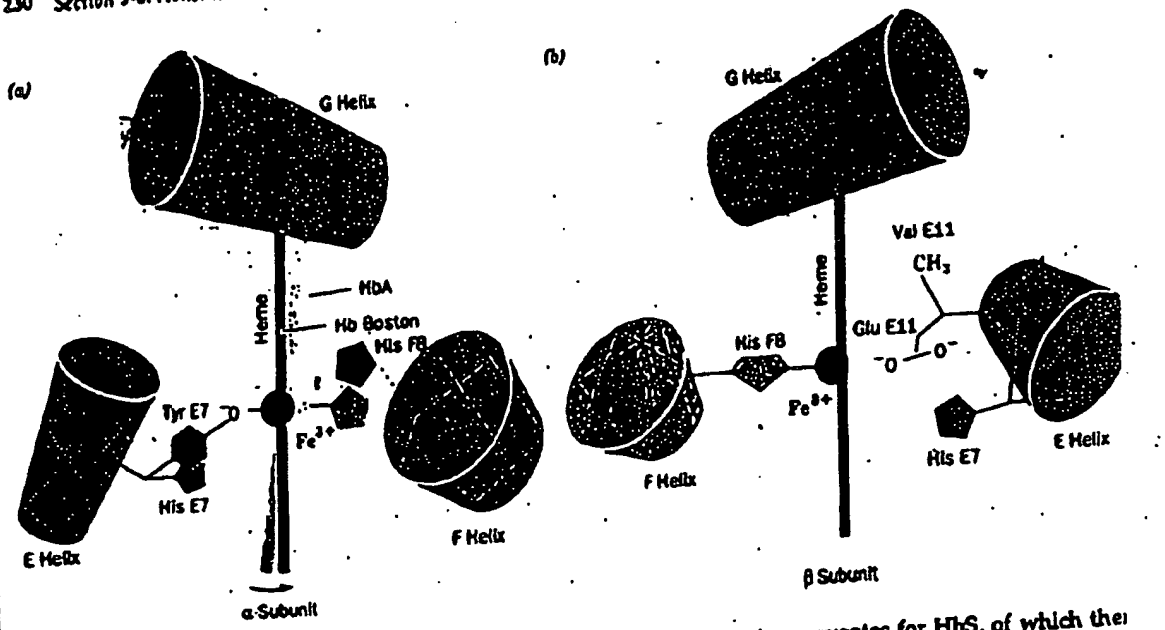

Figure 9-23
Mutations stabilizing the Fe(III) oxidation state of heme: (*a*) Alterations in the heme pocket of the α subunit on changing from deoxyHbA to Hb Boston [His E7(58)α → Tyr]. The phenolate ion of the mutant Tyr becomes the fifth ligand of the Fe atom thereby displacing the proximal His [F8(87)α]. [After Putsnelli, P. D., Perutz, M. F., and Nagel, R. L., *Proc. Natl. Acad. Sci.* 70, 3872 (1973).] (*b*) The structure of the heme pocket of the β subunit in Hb Milwaukee [Val E11(67)β → Glu]. Here the mutant Glu residue's carboxyl group forms an ion pair with the heme iron atom so as to stabilize its Fe(III) state. [From Perutz, M. F., Putsnelli, P. D., and Ranney, H. M., *Nature* 237, 260 (1972).]

pushes the subunits apart and displaces them towards the R state. This change shifts the T ⇌ R equilibrium almost entirely to the R state, which results in Hb Yakima having an increased O_2 affinity (P_{50} = 12 torr under physiological conditions vs 26 torr for HbA) and a total lack of cooperativity (Hill constant = 1.0). In contrast, the replacement of Asn G4(102)β by Thr in Hb Kansas eliminates the hydrogen bond in the α_1–β_2 contact that stabilizes the R state (Fig. 9-17*b*) so that this Hb variant remains in the T state upon binding O_2. Hb Kansas therefore has a low O_2 affinity (P_{50} = 70 torr) and a low cooperativity (Hill constant = 1.3).

B. Molecular Basis of Sickle-Cell Anemia

Most harmful Hb variants occur in only a few individuals, in many of whom the mutation apparently originated. However, ~10% of American blacks and as many as 25% of African blacks are heterozygotes for sickle-cell hemoglobin (HbS). HbS arises, as we have seen (Section 6-3A), from the substitution of a hydrophobic Val residue for the hydrophilic surface residue Glu A3(6)β (Fig. 9-13). The prevalence of HbS results from the protection it affords heterozygotes against malaria. However, homozygotes for HbS, of which there are some 50,000 in the United States, are severely afflicted by hemolytic anemia together with painful, debilitating, and sometimes fatal blood flow blockage caused by the irregularly shaped and inflexible erythrocytes characteristic of the disease.

HbS Fibers Are Stabilized by Intermolecular Contacts Involving Val β6 and Other Residues

The sickling of HbS-containing erythrocytes (Fig. 6-11) results from the aggregation (polymerization) of deoxy H. into rigid fibers that extend throughout the length of the c (Fig. 9-24). Electron microscopy indicates that the

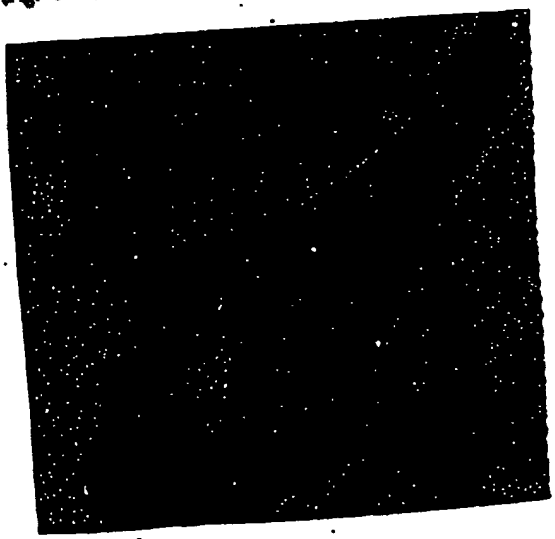

Figure 9-24
An electron micrograph of deoxyHbS fibers spilling out ruptured erythrocyte. [Courtesy of Robert Josephs, University of Chicago.]

Figure 9-25
220 Å in diameter fibers of deoxyHbS: (*a*) An electron micrograph of a negatively stained fiber. The accompanying cutaway interpretive drawing indicates the relationship between the inner and outer strands; the spheres represent individual HbS molecules. The fiber has a layer repeat distance of 64 Å and a moderate twist such that it repeats every 350 Å along the fiber axis. [Courtesy of Stuart Edelstein, University of Geneva.] (*b*) A cross-sectional diagram of the fiber indicating a probable pairing and polarity set for its 14 strands; differently shaded strands are antiparallel.

fibers are ~220 Å in diameter elliptical rods consisting of 14 hexagonally packed and helically twisting strands of deoxyHbS molecules that associate in parallel pairs (Figs. 9-25 and 9-26*a*).

The structural relationship among the HbS molecules in the pairs of parallel HbS strands has been established by the X-ray structure analysis of deoxyHbS crystals. When this crystal structure was first determined, it was unclear whether the intermolecular contacts in the crystal resembled those in the fiber. However, the subsequent observation that HbS fibers *slowly* convert to these crystals with little change in their overall X-ray diffraction pattern indicates that the fibers structurally resemble the crystals. The crystal structure of deoxyHbS consists of double filaments of HbS molecules whose several different intermolecular contacts are diagrammed in Fig. 9-26*b*. Only one of the two Val 6β's per Hb molecule contacts a neighboring molecule. In this contact, the mutant Val side chain occupies a hydrophobic surface pocket on an adjacent molecule's β subunit. This pocket, which is absent in oxyHb, is too small to contain HbA's Glu β6 side chain even if it was not hydrophilic (Fig. 9-26*c*). Other contacts involve residues that also occur in HbA including Asp 73β and Glu 23α (Fig. 9-26*b*). The observation that HbA does not aggregate into fibers, however, even at very high concentrations, indicates that *the contact involving Val 6β is essential for fiber formation.*

The importance of these other intermolecular contacts to the structural integrity of HbS fibers has been demonstrated by studying the effects of other mutant hemoglobins on HbS gelation (polymerization). For example, the doubly mutated Hb Harlem (Glu 6β → Val + Asp 73β → Asn) requires a higher concentration to gel than does HbS (Glu 6β → Val); similarly, mixtures of HbS and Hb Korle-Bu (Asp 73β → Asn) gel less readily than equivalent mixtures of HbS and HbA. This observation suggests that Asp 73β occupies an important intermolecular contact site in HbS fibers (Fig. 9-26*b*). Likewise, the observation that hybrid tetramers consisting of α subunits from Hb Memphis (Glu 23α → Gln) and β subunits from HbS gel less readily than does HbS indicates that Glu 23α also participates in the polymerization of HbS fibers (Fig. 9-26*b*). The other white-lettered residues in Fig. 9-26*b* have been similarly implicated in sticking interactions.

The Initiation of HbS Gelation Is a Complex Process

The gelation of HbS, both in solution and within the red cell, follows an unusual time course. A solution of HbS can be brought to conditions under which it will gel by lowering the pO_2, raising the HbS concentration, and/or raising the temperature. *Upon achieving gelation conditions, there is a reproducible delay that varies according to conditions from milliseconds to days. During this time, no HbS fibers can be detected.* Only after the delay do

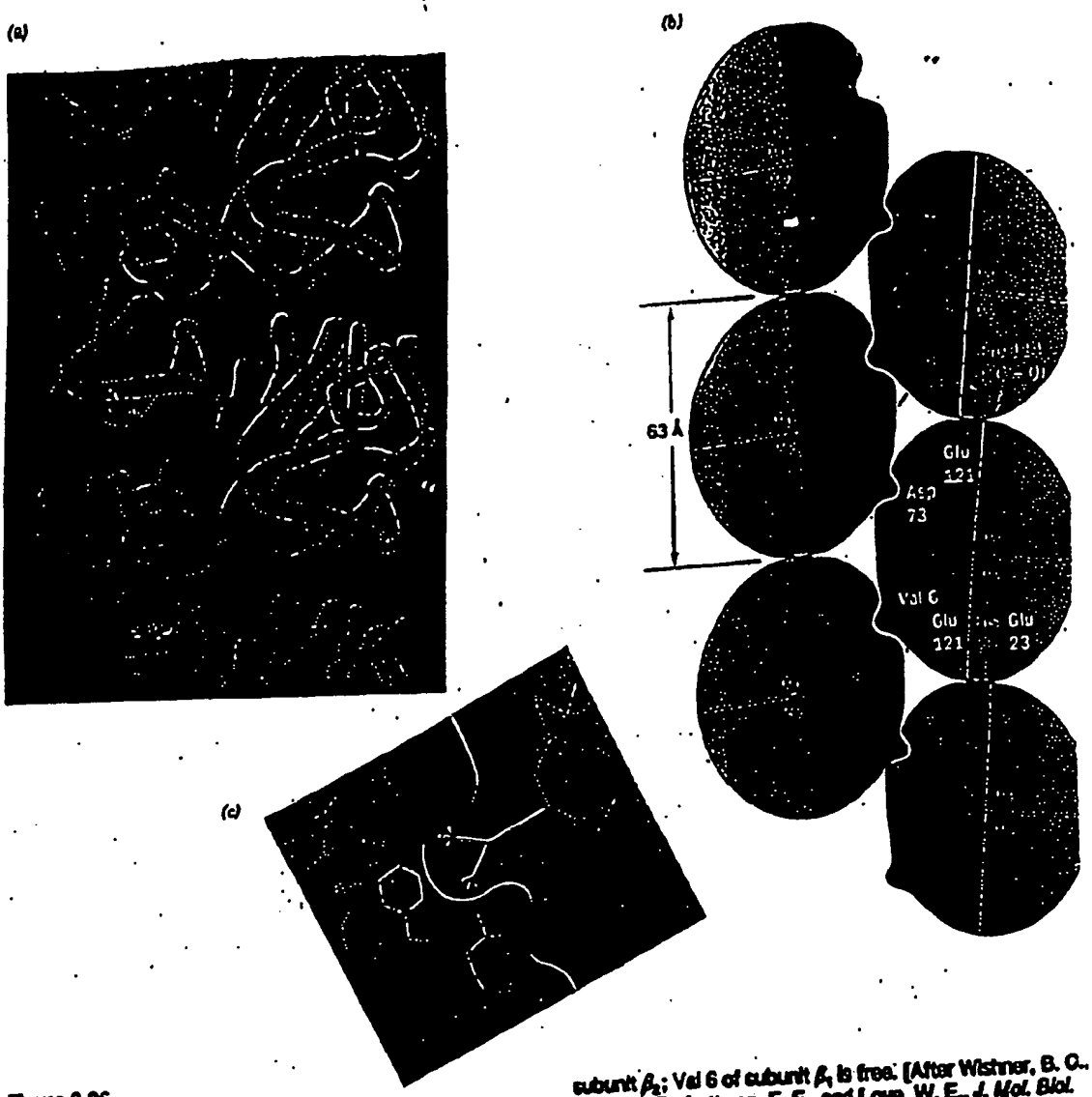

Figure 9-26
The structure of the deoxyHbS fiber. (a) The arrangement of the deoxyHbS molecules in the fiber. [Figure copyrighted © by Irving Geis.] (b) A schematic diagram indicating the intermolecular contacts in the crystal structure of deoxyHbS. The white-lettered residues are implicated in forming these contacts. Note that the only intermolecular association in which the mutant residue Val 6β participates involves subunit β_2; Val 6 of subunit β_1 is free. [After Wishner, B. C., Ward, K. B., Lattman, E. E., and Love, W. E., *J. Mol. Biol.* 98, 192 (1975).] (c) The mutant Val 6β_1 fits neatly into a hydrophobic pocket formed mainly by Phe 85 and Leu 88 c an adjacent β_1 subunit. This pocket, which is located between helices E and F at the periphery of the hem pocket, is absent in oxyHb and is too small to contain the normally occurring Glu 6β side chain. [Figure copyrighted © by Irving Geis.]

fibers first appear and gelation is then completed in about one half the delay time (Fig. 9-27*a*).

William Eaton and James Hofrichter discovered that the delay time, t_d, has a concentration dependence described by

$$\frac{1}{t_d} = k\left(\frac{c_t}{c_s}\right)^n \qquad [9.13]$$

where c_t is the total HbS concentration prior to gelation, c_s is the solubility of HbS measured after gelation is complete, and k and n are constants. Graphical analysis of the data indicates that $k \approx 10^{-7}\ s^{-1}$ and that n is between 30 and 50 (Fig. 9-27*b*). This is a remarkable result. *No other known solution process even approaches a 30 power concentration dependence.*

A two-stage process accounts for Eq. [9.13]:

1. At first, HbS molecules sequentially aggregate to form a nucleus consisting of m HbS molecules (Fig. 9-28*a*):

$$\text{HbS} \rightleftharpoons (\text{HbS})_2 \rightleftharpoons (\text{HbS})_3 \rightleftharpoons \cdots \rightleftharpoons (\text{HbS})_m -$$

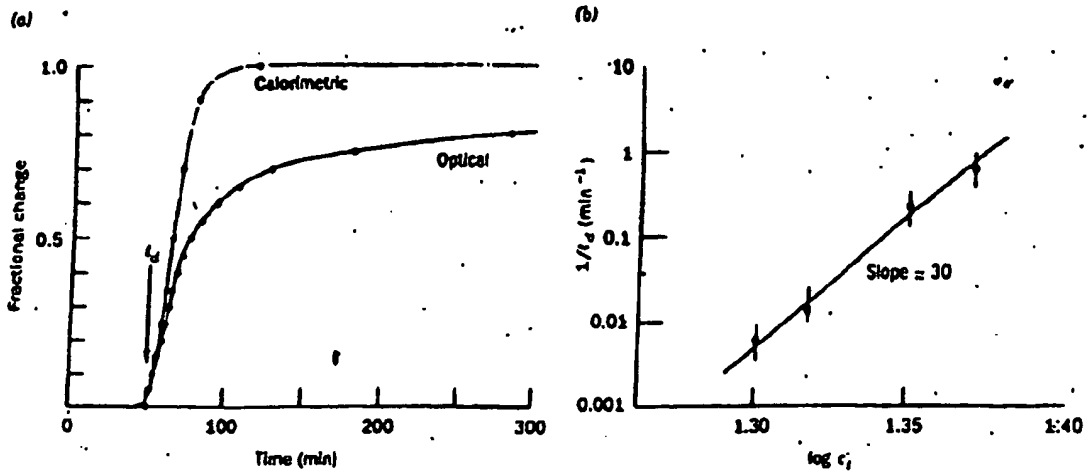

Figure 9-27
The time course of deoxyHbS gelation. (*a*) The extent of gelation as monitored calorimetrically (*yellow*) and optically (*purple*). Gelation of the 0.233 g·mL^{-1} deoxyHbS solution was initiated by rapidly increasing the temperature from 0°C, where HbS is soluble, to 20°C; t_d is the delay time. (*b*) A log–log plot showing the concentration dependence of t_d for the gelation of deoxyHbS at 30°C. The slope of this line is −30. [After Hofrichter, J., Ross, P. D., and Eaton, W. A., *Proc. Natl. Acad. Sci.* 71, 4865, 4867 (1974).]

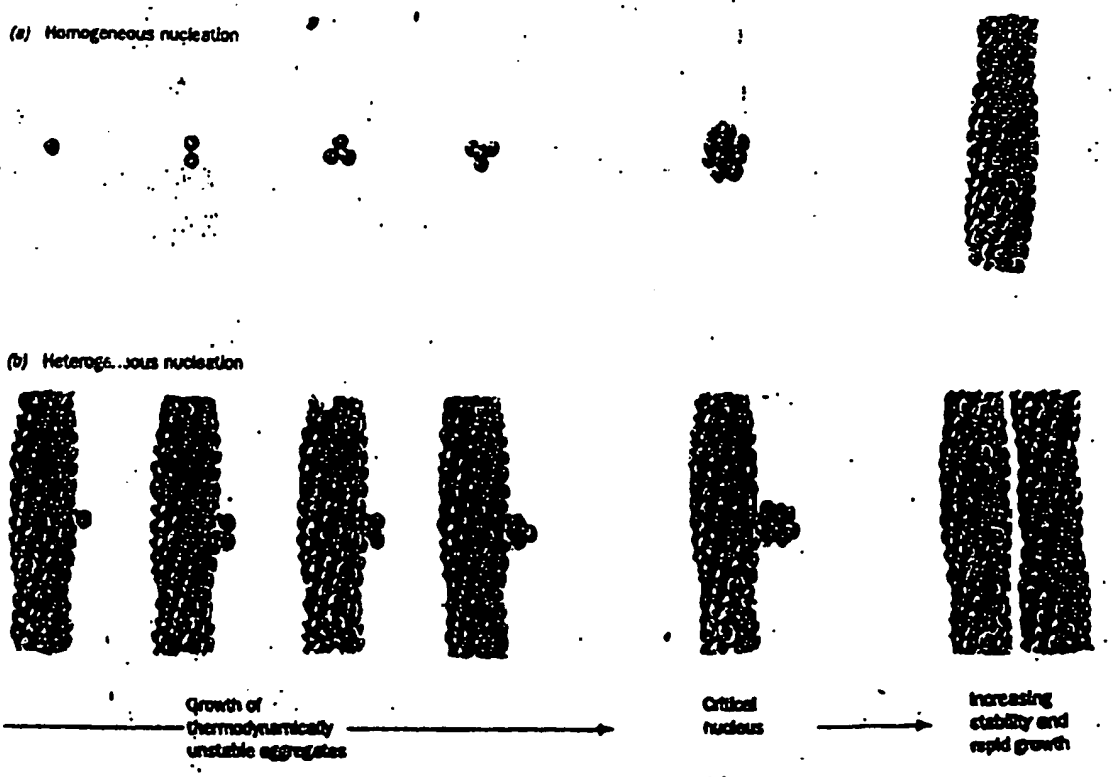

Figure 9-28
The double nucleation mechanism for deoxyHbS gelation: (*a*) The initial aggregation of HbS molecules (*circles*) occurs very slowly because this process is thermodynamically unfavorable and hence the intermediates tend to decompose rather than grow. However, once an aggregate reaches a certain size, the critical nucleus, its further growth becomes thermodynamically favorable leading to rapid fiber formation. (*b*) Each fiber, in turn, can nucleate the growth of other fibers leading to the explosive appearance of polymer. [After Ferrone, F. A., Hofrichter, J., and Eaton, W. A., *J. Mol. Biol.* 183, 614 (1985).]

Prenuclear aggregates are unstable and easily decompose, but once a nucleus has formed, it assumes a stable structure that rapidly elongates to form an HbS fiber.

2. Once a fiber has formed, it can nucleate the growth of other fibers (Fig. 9-28*b*). These newly formed fibers, in turn, nucleate the growth of yet other fibers, *etc.*, so that this latter process is autocatalytic.

The initial homogeneous nucleation process (taking place in solution) accounts for the very high concentration dependence in Eq. [9.13], whereas the secondary heterogeneous nucleation process (taking place on a surface—that of a fiber in this case) is responsible for the rapid onset of gelation (Fig. 9-27*a*).

The foregoing kinetic hypothesis suggests why sickle-cell anemia is characterized by episodic "crises" caused by blood flow blockages. HbS fibers dissolve essentially instantaneously upon oxygenation so that none are present in arterial blood. Erythrocytes take from 0.5 to 2 s to pass through the capillaries where deoxygenation renders HbS insoluble. If the delay time, t_d, for sickling is greater than this transit time, no blood flow blockage occurs (although sickling that occurs in the veins damages the erythrocyte membrane). However, Eq. [9.13] indicates that small increases in HbS concentration, c_t, and/or small decreases in HbS solubility, c_s, caused by conditions known to trigger sickle-cell crises, such as dehydration, O_2 deprivation, and fever, result in significant decreases of t_d. Once a blockage occurs, the resulting lack of O_2 and slow down of blood flow in the area compound the situation.

The kinetic hypothesis of sickling has profound clinical implications for the treatment of sickle-cell anemia. Heterozygotes of HbS, whose blood usually contains ~60% HbA and 40% HbS, rarely show any symptoms of sickling. The t_d for the gelation of their Hb is ~10^6-fold greater than that of homozygotes. Accordingly, a treatment of sickle-cell anemia that increases t_d by this amount, which corresponds to decreasing the ratio c_t/c_s by a factor of ~1.6, would relieve the symptoms of this disease. Three different therapeutic strategies to increase t_d, and thus inhibit HbS gelation, are under investigation:

1. The disruption of intermolecular interactions. Of particular interest are synthetic oligopeptides that have been designed with the aid of the X-ray structure of HbS to bind stereospecifically to its intermolecular contact regions.

2. The use of agents that increase hemoglobin's O_2 affinity. For example, the administration of cyanate carbamoylates the N-terminal amino groups of Hb (Fig. 9-21). This treatment eliminates some of the salt bridges that stabilize the T state (Section 9-2E) and thereby increases the O_2 affinity of Hb. Although cyanate is an effective *in vitro* antisickling agent, its clinical use has been discontinued because of toxic side effects, cataract formation and peripheral nervous system damage, that probably result from the carbamoylation of proteins other than Hb.

3. Lowering the HbS concentration (c_t) in erythrocytes. Agents that alter erythrocyte membrane permeability so as to permit the influx of water have promise in this regard.

Replacing HbS with other Hb molecules is also a promising possibility. Homozygotes for HbS with high levels of HbF in their blood, for example, have a relatively mild form of sickle-cell anemia. This observation has prompted the search for agents that can "switch on" the synthesis of HbF γ subunits in preference to that of the mutant HbS β subunits. The use of vasodilators (substances that dilate blood vessels) so as to reduce the entrapment of sickled erythrocytes in the capillaries may also relieve the symptoms of sickle-cell disease.

4. ALLOSTERIC REGULATION

One of the outstanding characteristics of life is the high degree of control exercised in almost all of its processes. Through a great variety of regulatory mechanisms, the exploration of which constitutes a significant portion of this text, an organism is able to respond to changes in its environment, maintain intra- and intercellular communications, and execute an orderly program of growth and development. Regulation is exercised at every organizational level in living systems, from the control of rates of reactions on the molecular level through the control of expression of genetic information on the cellular level, to the control of behavior on the organismal level. It is therefore not surprising that many, if not most, diseases are caused by aberrations in biological control processes.

Our exploration of the structure and function of hemoglobin continues with a theoretical discussion of the regulation of ligand binding to proteins through allosteric interactions (Greek: *allos*, other + *stereos*, solid; i.e., space). These cooperative interactions occur when the binding of one ligand at a specific site is influenced by the binding of another ligand, known as an effector or modulator, at a different (allosteric) site on the protein. If the ligands are identical, this is known as a homotropic effect, whereas if they are different, it is described as a heterotropic effect. These effects are termed positive or negative depending on whether the effector increases or decreases the protein's ligand-binding affinity.

Hemoglobin, as we have seen, exhibits both homotropic and heterotropic effects. The binding of O_2 results in a positive homotropic effect since it increases hemoglobin's O_2 affinity. In contrast, BPG, CO_2, and Cl^- are negative heterotropic effectors of O_2 binding to Hb because they decrease its affinity for O_2 (i.e.,

Proc. Natl. Acad. Sci. USA
Vol. 90, pp. 10056–10060, November 1993
Immunology

Molecular cloning and functional expression of a cDNA encoding glycosylation-inhibiting factor

(immunoregulation/macrophage migration inhibitory factor)

TOSHIFUMI MIKAYAMA*, TATSUHI NAKANO†, HIDEHO GOMI†, YUKIHITSU NAKAGAWA†, YUN-CAI LIU†, MASAHIRO SATO†, AKIHIRO IWAMATSU*, YASUYUKI ISHII*, WELSHUI Y. WEISER‡, AND KIMISHIGE ISHIZAKA†

†Division of Immunobiology, La Jolla Institute for Allergy and Immunology, La Jolla, CA 92037; ‡Department of Medicine, Harvard Medical School, Boston, MA 02115; and *Kirin Pharmaceutical Laboratory, Maebashi 371, Japan

Contributed by Kimishige Ishizaka, July 26, 1993

ABSTRACT By using probes based on partial amino acid sequence of glycosylation-inhibiting factor (GIF) from a mouse T-cell hybridoma, a full-length cDNA encoding mouse GIF was isolated. A cDNA clone encoding human GIF was isolated from cDNA libraries of a GIF-producing human T-cell hybridoma by using mouse GIF cDNA as a probe. The cDNAs encode a putative 12.5-kDa peptide of 115 amino acids. Northern blot analysis demonstrated a single, 0.6-kb transcript. Polyclonal rabbit antibodies against the *Escherichia coli*-derived recombinant 13-kDa peptide bound hybridoma-derived GIF. Although the peptide did not contain a signal peptide sequence, transfection of the cDNA into COS-1 cells resulted in secretion of 13-kDa peptide, but the peptide had substantially less bioactivity than the hybridoma-derived GIF. However, expression of a chimeric cDNA encoding a fusion protein consisting of the N-terminal pro region of calcitonin precursor and human GIF and cotransfection with furin cDNA to allow intracellular cleavage of the fusion protein resulted in secretion of 13-kDa peptide that was comparable to hybridoma-derived GIF in its bioactivity. Both the 13-kDa peptide and GIF bioactivity in the transfected COS-1 supernatant bound to a monoclonal antibody against hybridoma-derived human GIF. These results indicate that the 13-kDa peptide represents recombinant GIF, but posttranslational modification of the peptide is important for generation of the bioactivity. The GIF cDNA had high homology with the cDNA encoding macrophage migration inhibitory factor. However, the recombinant GIF failed to inhibit migration of human monocytes, and recombinant human macrophage migration inhibitory factor did not have GIF bioactivity.

Previous studies on regulation of IgE antibody response in rodents described glycosylation-inhibiting factor (GIF), a lymphokine that is involved in selective formation of IgE-suppressive factor (1). GIF inhibits N-glycosylation of IgE-binding factors (IgE-BFs), and the unglycosylated IgE-BFs then selectively suppress IgE synthesis. Subsequent experiments indicated that GIF facilitated the generation of antigen-specific suppressor T cells both *in vivo* (2) and *in vitro* (3) and provided evidence that GIF is a subunit of antigen-specific suppressor T-cell factors (TsFs) (4). This hypothesis is supported by the fact that the monoclonal antibody (mAb) against lipomodulin, 141-B9, binds not only GIF but also representative TsFs from hapten-specific suppressor T-cell hybridomas (5).

We expected that biochemical characterization and molecular cloning of GIF would help to solve controversial issues regarding antigen-specific TsFs. Mouse GIF (mGIF) was purified to homogeneity from serum-free culture supernatant of a representative GIF-producing T-cell hybridoma, 23IF1, by affinity chromatography on 141-B9-coupled immunosorbent (6). Subsequently, GIF-producing human T-cell hybridomas were established, and human GIF (hGIF) from a representative hybridoma, ACS, was identified as a 14-kDa peptide by SDS/PAGE (7). Based on these findings, the present experiments were undertaken to isolate cDNA clones that encode mGIF and hGIF.

MATERIALS AND METHODS

Purification of GIF. mGIF in serum-free culture supernatant of 23IF1 cells was purified by using Affi-Gel 10 (Bio-Rad) coupled to mAb 141-B9 (6) or coupled to the IgG fraction of a rabbit antiserum against recombinant mGIF. Recombinant hGIF was fractionated on Affi-Gel 10 coupled to the anti-hGIF mAb 38IF1 (7). Usually, 2–5 mg of a mAb or 10 mg of IgG from rabbit antiserum was coupled to 1 ml of gel. Procedures for the fractionation have been described (6, 7). After recovery of the flow-through fraction, the immunosorbent was washed with 20 column volumes of phosphate-buffered saline (0.05 M phosphate/0.15 M NaCl, pH 7.0), and proteins retained in the column were recovered by elution with 0.1 M glycine/HCl buffer (pH 3.0).

Recombinant mGIF expressed in *Escherichia coli* was purified from inclusion bodies. After disruption of *E. coli* cells, the pellet fraction was extracted with 0.2 M Tris·HCl buffer (pH 8.0) containing 6 M guanidine hydrochloride and 25 mM EDTA, and the extract was fractionated on a Sephacryl S-200 column equilibrated with the same buffer. Fractions containing the 13-kDa peptide, detected by SDS/PAGE, were concentrated and slowly added to a large volume of Tris buffer for refolding of peptides. The sample was then applied to a TSK gel DEAE-5PW column (Toyo Soda, Tokyo) equilibrated with 20 mM Tris·HCl buffer (pH 8.0), and proteins were eluted with a gradient of 0–0.1 M NaCl.

Amino Acid Sequencing. Affinity-purified mGIF was precipitated by 10% (wt/vol) trichloroacetic acid (6), electrophoresed in an SDS/15% polyacrylamide gel under reducing conditions, and then electroblotted to a poly(vinylidene difluoride) (PVDF) membrane. The immobilized 13-kDa protein was reduced and S-carboxymethylated *in situ* (8) and digested with 1 pM *Achromobacter* protease I (Wako Pure Chem., Tokyo) at pH 9.0. Peptides retained on PVDF membranes were subdigested with 2 pM endoproteinase Asp-N

Abbreviations: GIF, glycosylation-inhibiting factor; mGIF, mouse GIF; hGIF, human GIF; IgE-BF, IgE-binding factor; mAb, monoclonal antibody; TsF, suppressor T-cell factor; MIF, macrophage migration inhibitory factor; pro-CT, pro region of calcitonin precursor; PVDF, poly(vinylidene difluoride).

The sequences reported in this paper have been deposited in the GenBank data base (accession nos. 10612 (hGIF) and 10613 (mGIF)).

The publication costs of this article were defrayed in part by page charge payment. This article must therefore be hereby marked "advertisement" in accordance with 18 U.S.C. §1734 solely to indicate this fact.

(Boehringer Mannheim) in 100 mM ammonium bicarbonate (pH 7.8) containing 8% acetonitrile. Peptides released from the membrane after each digestion were fractionated by reverse-phase HPLC on a μBondapak C_{18} column (particle size, 5 μm; pore size, 300 Å; Waters) equilibrated with 0.05% trifluoroacetic acid as a mobile phase. Peptides were eluted by a linear gradient (0–50%) of 0.025% trifluoroacetic acid in 2-propanol/acetonitrile, 7:3 (vol/vol). Amino acid sequence analysis of each peptide was performed with a gas-phase sequencer (Applied Biosystems, model 470A) with modified programs for microsequencing (17).

Construction of cDNA Library. Total cellular RNA was isolated from 23IF1 cells (4) or ACS cells (7) by using RNAzol (Tel-Test, Friendswood, TX). Poly(A)$^+$ RNA was isolated by using a FastTrack mRNA isolation kit (Invitrogen). cDNA libraries were constructed with a Uni-Zap cDNA synthesis kit (Stratagene). After screening of the cDNA library, selected cDNA clones were sequenced by the standard dideoxy method with the Sequenase kit (United States Biochemical). The DNA sequences were analyzed with MACVECTOR software (International Biotechnologies).

Expression of Recombinant GIF. For bacterial expression of mGIF, *Afl* II and *Bam*HI adaptor sites were ligated at both ends of mGIF cDNA by polymerase chain reaction (PCR), and the cDNA fragment was inserted by ligation into pSTH1 vector (18) carrying the *trp* promoter and *trpA* terminator. The plasmid was transformed into competent *E. coli* RR1 cells, and the cells carrying plasmid were cultured in M9 broth with glucose (0.8%), amino acids (0.4%), thiamin (10 μg/ml), and ampicillin (50 μg/ml). Cells were harvested 5 hr after the addition of indoleacrylic acid (11).

For the expression of GIF cDNA in COS-1 cells, two different types of plasmids were constructed. In one type, mGIF or hGIF cDNA was ligated into *Bgl* II/*Kpn* I-digested modified SRα vector (11). Since GIF does not appear to have a signal peptide sequence, we constructed another expression system for translation of a fusion protein which consisted of the N-terminal pro region of the human calcitonin precursor (pro-CT) and human GIF. Intracellular cleavage of the fusion protein was mediated by an endoprotease, furin (13), allowing the secretion of mature GIF peptide (14). The cDNA fragment encoding pro-CT was amplified by PCR using a human calcitonin cDNA as the template and oligonucleotide primers tailed with a *Pst* I recognition site (14). The amplified gene was cloned into the SRα vector at the *Pst* I site. To fuse hGIF cDNA to the 3′ end of pro-CT cDNA in frame, the 5′ extension method was applied to hGIF cDNA. The sequence of the 5′ primer was 5′-GCAGATCTAAGCGGATGCCGATGTTCATGGTAAACACC-3′, which contains a *Bgl* II site (see Fig. 1*B*). The amplified hGIF gene was ligated into *Bgl* II/*Kpn* I-digested SRα vector in which pro-CT cDNA had been inserted. Human furin cDNA was cloned into the SRα vector as described (14). The plasmids were transfected into COS-1 cells either by the DEAE-dextran method or by electroporation. After transfection, cells were incubated overnight in a 1:1 mixture of Dulbecco's modified Eagle's medium and Ham's nutrient mixture F12 (DMEM/F12) containing 10% fetal bovine serum and then were cultured for 1 week in serum-free DMEM/F12 containing bovine insulin (20 μg/ml; Sigma), human transferrin (20 μg/ml; Sigma), 40 μM monoethanolamine, 0.1 μM sodium selenite, and bovine serum albumin (1 mg/ml; Sigma) to recover culture supernatant.

Electrophoresis and Immunoblotting. Affinity-purified GIF preparations were analyzed by SDS/PAGE in a 15% polyacrylamide slab gel under reducing conditions (15), and proteins in the gel were visualized by silver staining (16). An aliquot of a sample was analyzed along with serial 2-fold dilutions of *E. coli*-derived recombinant mGIF of known concentrations, and the concentration of the 13-kDa peptide in the sample was estimated by the intensity of the band in silver staining. Immunoblotting was carried out with the enhanced chemiluminescence (ECL) Western blot detection system (Amersham). Polyclonal rabbit antibodies against recombinant mGIF were affinity-purified by absorption of the IgG fraction of the anti-GIF antiserum with Affi-Gel 10 coupled to *E. coli*-derived mGIF, and proteins retained in the column were eluted with glycine-HCl buffer (pH 3.0). Two to 4 μg/ml of the affinity-purified antibodies was used to detect the GIF band.

Detection of GIF Bioactivity. GIF was detected by its ability to switch the mouse T-cell hybridoma 12H5 cells from the formation of glycosylated IgE-BF to the formation of ungly-cosylated IgE-BF. Detailed procedures for the assay have been described (3). Briefly, the 12H5 cells were cultured with mouse IgE (10 μg/ml) in the presence or absence of a test sample, and IgE-BF in culture filtrates was fractionated on lentil lectin-Sepharose. When the 12H5 cells were cultured with IgE alone, essentially all IgE-BF formed by the cells bound to lentil lectin-Sepharose and was recovered by elution with methyl α-D-mannoside. When a sufficient amount of GIF was added to the 12H5 cells together with IgE, a majority of the IgE-BF formed by the cells was not retained in the column and was recovered in the effluent fraction (3).

Assay for Macrophage Migration Inhibitory Factor (MIF). Human peripheral blood monocytes were employed as indicator cells in an agarose-droplet assay system (17). The assay was set up in triplicate or quadruplicate together with serial dilutions of a supernatant of COS-1 cells transfected with MIF cDNA (18) as a positive control. The area of migration was calculated by the following formula: migration = (diameter of total area/diameter of agarose droplet)^2 − 1. Percent inhibition = 100 − [(average migration of test sample/average migration of negative control) × 100]. In this assay, inhibition of ≥20% was considered to be significant (19).

RESULTS

cDNA Cloning of GIF. mGIF was isolated from culture supernatant of 23IF1 cells, and the 13-kDa peptide immobilized on PVDF membrane was employed for determination of partial amino acid sequence. In this experiment, we obtained six different peptides consisting of 13–15 amino acids. Based on the N-terminal amino acid sequence (MPMFTVNTNV-PRASV) and the sequence of one of the fragments (DPCALCSLHSIGK), oligonucleotides were synthesized, and PCR was carried out using the two oligonucleotides as primers and single-stranded cDNA of 23IF1 cells as the template. A 0.2-kb fragment amplified in the PCR was ligated to pCR1000 vector for subsequent cloning and DNA sequencing. After the nucleotide sequence was confirmed, the 0.20-kb fragment was used to screen a cDNA library from 23IF1 cells.

Seven cDNA clones were isolated after screening of 0.5 × 10^6 independent clones. Since restriction mapping of all of the cDNA clones showed a single pattern, the longest clone, with an insert of 0.6 kb, was chosen for DNA sequencing. The nucleotide sequence and deduced amino acid sequence of mGIF are shown in Fig. 1*A*. The largest open reading frame encodes 115 amino acids and the predicted amino acid sequence contained all six peptides obtained by Edman degradation of purified mGIF. The calculated size of the GIF protein is 12.5 kDa, which is in good agreement with that of purified mGIF (6). The nucleotide sequence flanking the first methionine codon favors the translation initiation rule (21). The amino acid sequence downstream from this methionine has a perfect match to that of the N-terminal sequence of the purified GIF, suggesting that GIF has no signal peptide sequence.

Since high homology was expected between mGIF and hGIF, a cDNA library constructed from mRNA of a human

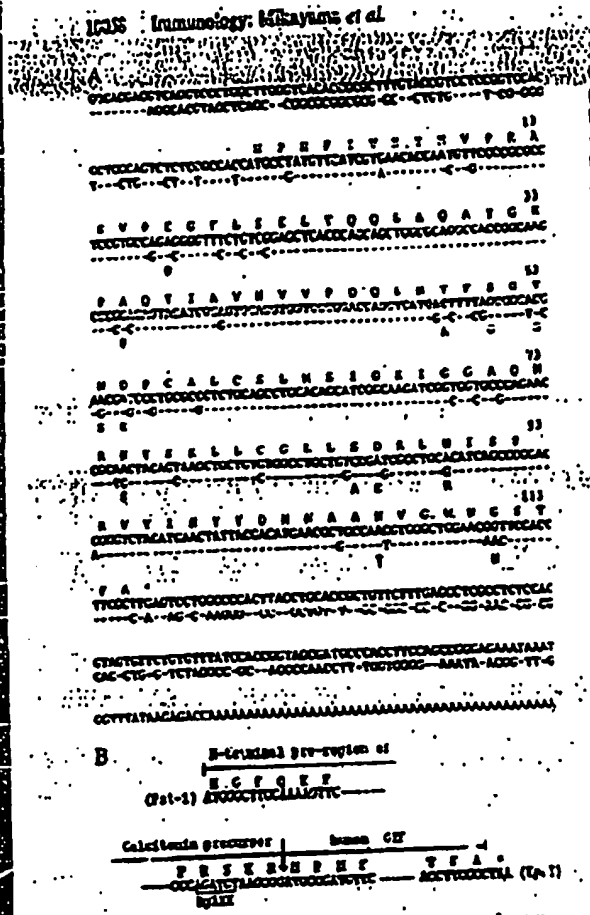

FIG. 1. (A) Structure of GIF cDNA clones. The second line shows the full-length nucleotide sequence of a mGIF cDNA clone, and the first line shows the predicted amino acid sequence of mGIF. The third and fourth lines show the nucleotide and amino acid sequences, respectively, of a human cDNA clone. Only differences from the mGIF sequence are shown. Arrow indicates the only difference between hGIF cDNA and human MIF cDNA, which has AGT (serine). Six peptides obtained from 231F1-derived 13-kDa GIF corresponded to amino acids 1–15, 13–36, 57–67, 63–78, 86–100, and 101–115 in the deduced amino acid sequence of mGIF. (B) Nucleotide sequence of the insert encoding a fusion of pro-CT with hGIF. Deduced amino acid sequence is shown above the nucleotide sequence. The recognition motif for furin is Arg-Xaa-Lys-Arg (20). The cleavage site is shown by an arrow. The insert was ligated into 5Rα vector through *Pst* I and *Kpn* I sites, as indicated in parentheses.

GIF-producing hybridoma, ACS, was screened with the mGIF cDNA as a probe. Among 27 clones hybridized, 4 clones having a 0.5-kb insert were sequenced, and the structure was compared with that of mGIF (Fig. 1A). The hGIF and mGIF sequences were 80% identical at the whole cDNA level, 89% identical in the putative coding region, and 90% identical at the amino acid level. The sequence of the coding region of hGIF cDNA was almost identical to the sequence of human MIF cDNA (18). The only difference is that amino acid 106 of MIF is serine, whereas the corresponding residue of hGIF is asparagine (see Fig. 1A).

The expression and the size of transcripts that hybridized to hGIF cDNA were examined by Northern analysis. Surprisingly, GIF mRNA was detected in all of the mouse cell line cells tested—231F1, CTLL-2, BW5147, A20.3, and NIH 3T3 (fibroblast). Various human cell line cells such as ACS, CEM, RPMI8866, WI-38 (embryonic fibroblast), and PC3 (prostate carcinoma cells) also contained mRNA which hybridized to the hGIF cDNA. Only a single transcript of 0.6 kb was observed in mouse or human cell line (Fig. 2). Northern blotting of RNAs from mouse tissues showed a dominant expression of GIF mRNA in brain, liver, and kidney. Since the size of the transcript is close to the size of the GIF cDNA (584 bp), it is likely that the mGIF and hGIF clones isolated represent full-length cDNAs of GIF.

Isolation of Hybridoma-Derived GIF by Use of Antibodies Against Recombinant 13-kDa Peptide. If the cDNA clones actually encode GIF, one may expect that antibodies against recombinant 13-kDa peptide will bind GIF from T-cell hybridomas. To test this possibility, rabbit antibodies against the *E. coli*-derived 13-kDa peptide were obtained. The purity of the recombinant mouse peptide employed for immunization was >95% as determined by SDS/PAGE (Fig. 1A), and the N-terminal amino acid sequence of the peptide corresponded to that predicted from the nucleotide sequence of the cDNA. Rabbits were immunized by an intramuscular injection of 100 μg of peptide included in complete Freund's adjuvant, and the antiserum was obtained after five booster injections. Since IgG at 2–4 μg/ml in the antiserum was adequate for detection of the recombinant 13-kDa peptide by Western blotting, culture filtrate of the 231F1 cells was fractionated on Affi-Gel 10 coupled with the IgG fraction of the antiserum. GIF activity was not detectable in the flow-through fraction, and >80% of the bioactivity in the culture filtrate was recovered in the eluate fraction, which gave a 13-kDa band upon SDS/PAGE (Fig. 1A). Estimation of the concentration of the 13-kDa peptide in the eluate fraction indicated that a peptide concentration of 5 ng/ml was sufficient for detection of GIF bioactivity (Table 1). Similar experiments were carried out with culture supernatants of a GIF-producing human T-cell hybridoma. Essentially all GIF activity in the supernatant bound to the anti-GIF Affi-Gel and was recovered by acid elution. The minimum concentration

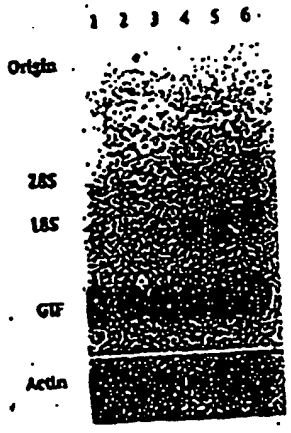

FIG. 2. Expression of the 0.6-kb GIF transcript. Lanes: 1, 231F1; 2, BW5147 (thymoma); 3, CTLL-2 (cytotoxic T-cell line); 4, A20.3 (B-cell line); 5, PT-58 (mouse mast cell line); 6, NIH 3T3 (fibroblast line). Samples (10 μg) of cellular RNA were electrophoresed in formaldehyde/1% agarose gel and blotted to a charged nylon membrane. After probing with the ^{32}P-labeled mGIF cDNA, the same membrane was stripped and hybridized with a PCR-amplified ~~cDNA~~ cDNA labeled with ^{32}P under the same conditions. Conditions for hybridization were 50% formaldehyde/5X standard saline citrate (SSC)/1× Denhardt's solution/0.5% SDS at 42°C, followed by subsequent washing with 2× SSC/0.1% SDS at 25°C and 0.5× SSC/0.1% SDS at 65°C. Positions of 28S and 18S rRNA are shown.

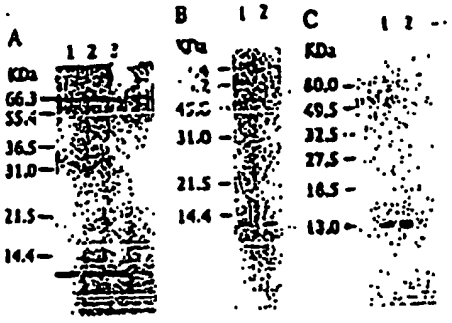

FIG. 3. Identification of hybridoma-derived GIF and recombinant GIF by SDS/PAGE. (*A*) Comparison among *E. coli*-derived mGIF, 2H1F1-derived mGIF, and GIF from COS-1 cells transfected with mGIF cDNA. *E. coli*-derived mGIF, isolated from inclusion bodies, was applied to lane 1. The 2H1F1-derived GIF (lane 2) and COS-1-derived GIF (lane 3) were purified by using Affi-Gel 10 coupled to polyclonal antibodies against recombinant mGIF. Supernatant of COS-1 cells transfected with SRα vector alone was absorbed with the same immunosorbent, and the acid eluate fraction was applied to lane 4. Peptides were detected by silver staining. (*B* and *C*) Recombinant hGIF expressed in COS-1 cells. Mature 13-kDa GIF was detected by silver staining (*B*) and by Western blotting (*C*). hGIF cDNA ligated into SRα vector was transfected into COS-1 cells, and recombinant GIF in COS-1 supernatant was purified on $3BF_1$-Affi-Gel (lane 1). hGIF was expressed by cotransfection of a chimeric cDNA encoding pro-CT-hGIF fusion protein and furin cDNA and was purified by the same procedure (lane 2).

of the 13-kDa peptide required for the detection of GIF activity in the eluate fraction was estimated to be 10 ng/ml (Table 1).

Production of Bioactive Recombinant GIF in COS-1 Monkey Cells. The mGIF cDNA was ligated into a modified SRα vector, and the plasmid was transfected into COS-1 cells. Culture supernatant of the transfected cells contained GIF bioactivity and the 13-kDa peptide, which was detected by Western blotting using polyclonal anti-GIF antibodies. Supernatants from GIF-transfected COS-1 cells and from mock-transfected cells were fractionated with the anti-GIF coupled to Affi-Gel. Essentially all GIF bioactivity in the supernatant of GIF-transfected cells bound to the immunosorbent and was recovered by acid elution, whereas the activity was not detectable in the acid eluate fraction of the supernatant from mock transfectants. The 13-kDa peptide was detected in the eluate of GIF-transfected COS supernatant but barely detectable in the fraction from mock-transfected cells (Fig. 3*A*). The hGIF cDNA was expressed in COS-1 cells using the same vector, and the supernatants were fractionated on $3BF_1$-Affi-Gel. As expected, all GIF bioactivity in the culture supernatant of GIF-transfected cells bound to the immunosorbent and was recovered by acid elution. The acid eluate fraction gave a 13-kDa band upon SDS/PAGE (Fig. 3*B*), and polyclonal anti-GIF antibodies bound to the band on a Western blot (Fig. 3*C*). These results collectively indicate that the 13-kDa peptide formed by transfected cells has GIF bioactivity. However, titration of GIF bioactivity in the affinity-purified recombinant mGIF and hGIF and estimation of the concentration of 13-kDa peptide in the preparations by SDS/PAGE indicated that the concentration of recombinant GIF required for the detection of GIF activity was 150–250 ng/ml (Table 1).

Quantitative difference in the biologic activities between the hybridoma-derived GIF and recombinant GIF suggested to us the possibility that bioactivity of the 13-kDa peptide may depend on posttranslational modification of the peptide. Since GIF does not have a signal peptide (Fig. 1*A*), we applied a device for the secretion of a recombinant truncated peptide via the constitutive pathway (14). Our approach was to fuse the cDNA fragment encoding human pro-CT with GIF-cDNA for the expression of a fusion protein in COS-1 cells and to utilize furin for intracellular cleavage of the fusion protein and subsequent secretion of the mature GIF. The nucleotide sequence of the insert encoding the fusion protein and the predicted amino acid sequence around the cleavage site are shown in Fig. 1*B*. Indeed, cotransfection of the cDNA encoding the fusion protein and furin cDNA resulted in secretion of the 13-kDa GIF. Bioactivity of the supernatant was 5–10 times higher than that of COS-1 cells transfected with hGIF cDNA. The supernatant contained the 13-kDa peptide, which could be affinity-purified by $3BF_1$-Affi-Gel, and the peptide band in SDS/PAGE bound polyclonal anti-GIF on a Western blot (Fig. 3 *B* and *C*). As expected, essentially all GIF bioactivity in the culture supernatant was recovered in the acid eluate fraction from $3BF_1$-Affi-Gel. Further fractionation of the eluate on polyclonal anti-GIF coupled Affi-Gel indicated that both the 13-kDa peptide and the GIF bioactivity in the fraction bound to the antibodies and were recovered by acid elution. It was also found that GIF activity in the original culture supernatant bound to anti-lipocortin (41-B9)-coupled Affi-Gel. Titration of GIF bioactivity in the affinity-purified GIF preparations showed that the specific bioactivity of recombinant hGIF obtained by this method was comparable to that of hybridoma-derived GIF (Table 1).

Since the GIF cDNA has high homology to MIF cDNA (15), we determined MIF activity of recombinant GIF. Culture supernatant of COS-1 cells cotransfected with pro-CT-hGIF cDNA and furin cDNA was fractionated on $3BF_1$-Affi-Gel, and both the effluent and acid eluate fractions were assessed for MIF activity and GIF activity. Neither the effluent nor eluate fraction had MIF activity, although GIF bioactivity was detected in a 1:100 dilution of the eluate fraction. In the same assay, supernatant of COS-1 cells transfected with MIF cDNA showed MIF activity at the final dilution of 1:10, but no GIF activity was detected in a 1:4 dilution of the supernatant.

Table 1. Bioactivity of hybridoma-derived GIF and recombinant (r) GIF

Purified GIF	Cell source	Antibody used for purification	13-kDa peptide for GIF activity,* ng/ml
mGIF	2H1F1	Anti-GIF	5
hGIF	3H9	Anti-GIF	10
rmGIF	COS-1	Anti-GIF	250
rhGIF	COS-1	$3BF_1$	150
rhcGIF†	COS-1	$3BF_1$	10
		Anti-GIF	5
		41-B9	10

GIF in culture supernatant was purified by using Affi-Gel immunosorbent coupled either to polyclonal anti-recombinant mGIF (anti-GIF) or with mAb against hybridoma-derived GIF ($3BF_1$), or monoclonal anti-lipocortin (41-B7).

*Minimum concentration of the 13-kDa peptide required for the detection of GIF bioactivity. These values were calculated from the concentration of the 13-kDa peptide in an affinity-purified GIF and GIF bioactivity in serial 2-fold dilutions of the purified preparations.

†Recombinant hGIF obtained by cotransfection of a chimeric cDNA encoding a pro-CT-hGIF fusion protein and furin cDNA.

DISCUSSION

In this paper, we describe the molecular cloning of cDNAs coding for mGIF and hGIF. Both cDNA clones contain a single open reading frame of 345 nucleotides which encodes a peptide of 115 amino acids. The predicted amino acid

sequence of mGIF was exactly the same as that of a growth factor-induced delayed early response gene (22), and the nucleotide sequence of hGIF cDNA was identical to that of MIF cDNA (16), except for one base (Fig. 1A). The hydropathicity plot of the amino acid sequences of both mGIF and hGIF revealed that hydrophobic and hydrophilic regions are clearly separated and that the length of each region is 20–25 residues. This finding suggests that GIF is a globular protein and that three-dimensional structure of the molecules may be important for their biologic function.

Important findings from the biologic viewpoint were (*i*) that transfection of the GIF cDNA into COS-1 cells resulted in the secretion of bioactive 13-kDa peptide and (*ii*) that the recombinant GIF bound to both the mAb against hybridoma-derived GIF and anti-lipomodulin, while the polyclonal antibodies against recombinant mouse 13-kDa peptide specifically bound hybridoma-derived mGIF and hGIF. When one considers the 90% identity in amino acid sequence between mGIF and hGIF, cross-reaction of the antibodies with hGIF is reasonable. Furthermore, bioactivity of the recombinant 13-kDa peptide which was obtained by cotransfection of the chimeric gene encoding a pro-CT-hGIF fusion protein and furin cDNA was comparable to that of hybridoma-derived GIF. These findings collectively indicate that the recombinant 13-kDa peptide actually represents GIF. However, the 13-kDa peptide obtained by transfection of either mGIF cDNA or hGIF cDNA alone was 10- to 30-fold less active than the hybridoma-derived GIF. Since GIF does not have a signal peptide, one may predict that the recombinant 13-kDa peptide synthesized in this system will not go through the endoplasmic reticulum. Mechanisms underlying the secretion of soluble factors without signal peptides—interleukins 1α and 1β—remain unclear (23). Nevertheless, the pro-CT-GIF fusion protein synthesized in COS-1 cells will go through the endoplasmic reticulum and Golgi apparatus, where the fusion protein is cleaved by the furin coexpressed in these cells (13). One may speculate that posttranslational modification of the 13-kDa peptide—e.g., proper folding of the peptide, intrachain disulfide formation, or phosphorylation—is important for the generation of GIF bioactivity. This idea may explain the fact that essentially all cell line cells and mouse tissues contained mRNA for GIF (Fig. 2), whereas the major cell source of bioactive GIF is limited to certain subsets of lymphocytes (1). It has been shown that Lyt-2$^+$ splenic T lymphocytes and antigen-specific murine suppressor T hybridomas secreted bioactive GIF but that helper T-cell clones and hybridomas did not. Our recent experiments showed that the murine CD4$^+$ T-cell hybridoma 12H5 and human CD4$^+$ T-cell line CEM secreted the 13-kDa peptide which reacted with polyclonal anti-GIF; however, even at 0.5–1.0 μg/ml, the peptide from these cells did not exert GIF bioactivity. One might speculate that the 13-kDa peptide translated in suppressor T cells is modified for the secretion of bioactive GIF, while similar posttranslational modification of the peptide does not occur in helper T cells. Elucidation of the mechanisms for the formation and secretion of bioactive 13-kDa peptide by suppressor T cells requires further studies.

High amino acid sequence homology between hGIF and MIF suggested that GIF might have MIF activity. However, our experiments showed that affinity-purified recombinant hGIF failed to inhibit migration of human monocytes even at a 20-fold higher concentration than that required for the detection of GIF activity. It was also found that affinity-purified mGIF from 231F1 cells, with a GIF titer of 1:50, failed to inhibit the migration of mouse macrophages (results not shown). In contrast, the supernatant of COS-1 cells transfected with MIF cDNA showed a high MIF activity but did not have GIF activity. Our more recent experiments indicated that MIF activity in the supernatant failed to be retained in either 18BF$_1$-coupled Affi-Gel or polyclonal anti-GIF-coupled Affi-Gel. The results collectively indicate that GIF is distinct from MIF. Since recombinant MIF has not been affinity-purified, it is not conclusive that the 13-kDa peptide of the predicted amino acid sequence has the MIF activity. At present, however, the possibility cannot be excluded that a single amino acid difference between GIF and MIF may account for their biologic activities. Lanahan *et al.* (22) reported that the cDNA probe of a growth factor-induced delayed early response gene, which has exactly the same sequence as our mGIF cDNA, hybridized with a large number of murine and human genomic restriction fragments, suggesting that there is a family of MIF-like genes. The GIF gene appears to belong to this family but is distinct from the MIF gene.

This paper is publication no. 79 from the La Jolla Institute for Allergy and Immunology. This work was supported by Research Grants AI11297 and AI14784 from the U.S. Department of Health and Human Services.

1. Ishimaru, K. (1984) *Annu. Rev. Immunol.* 2, 159–182.
2. Akasaki, M., Jardieu, P. & Ishimaru, K. (1986) *J. Immunol.* 136, 3172–3179.
3. Iwata, M. & Ishimaru, K. (1988) *J. Immunol.* 141, 3270–3277.
4. Jardieu, P., Akasaki, M. & Ishimaru, K. (1987) *J. Immunol.* 138, 1494–1501.
5. Steele, I. K., Kuchroo, V. K., Kawasaki, H., Jayaraman, S., Iwata, M., Ishimaru, K. & Dorf, M. E. (1989) *J. Immunol.* 143, 2213–2220.
6. Tagaya, Y., Mori, A. & Ishimaru, K. (1992) *Proc. Natl. Acad. Sci. USA* 89, 9117–9121.
7. Thomas, P., Gomi, H., Takeuchi, T., Curiel, C., Tagaya, Y. & Ishimaru, K. (1992) *J. Immunol.* 148, 729–737.
8. Iwamatsu, A. (1992) *Electrophoresis* 13, 142–147.
9. Iwamatsu, A., Aoyama, H., Dibo, G., Tamamura, S. & Sakiyama, F. (1991) *J. Biochem. (Tokyo)* 110, 153–158.
10. Matsuki, S., Ozawa, T., Nagao, S., Hirata, H., Kaneko, H. & Nozawa, Y. (1990) *Biotechnol. Appl. Biochem.* 12, 284–291.
11. Nicholl, D. P. G. & Yeaddiy, C. (1987) *Methods Enzymol.* 155, 155–164.
12. Takabe, Y., Schild, M., Fellerman, L., Hoy, P., Yokota, K., Arai, K., Yoshida, M. & Arai, N. (1988) *Mol. Cell. Biol.* 8, 466–472.
13. Wise, R. J., Barr, P. J., Wong, P. A., Kiefer, M. C., Brake, A. J. & Kaufman, R. J. (1992) *Proc. Natl. Acad. Sci. USA* 89, 9378–9382.
14. Liu, Y.-C., Kawasaki, H., Mikayama, T., Isogai, Y., Takeuchi, T. & Obata, H. (1991) *Proc. Natl. Acad. Sci. USA* 88, 8957–8961.
15. Laemmli, U. K. (1970) *Nature (London)* 227, 680–685.
16. Oakley, B. R., Kirsch, D. R. & Morris, N. R. (1980) *Anal. Biochem.* 105, 361–363.
17. Renold, H. G. & Merrifield, A. D. (1985) *Methods Enzymol.* 116, 379–394.
18. Weiser, W. Y., Temple, P. A., Witek-Giannotti, J. S., Remold, H. G., Clark, S. C. & David, J. R. (1989) *Proc. Natl. Acad. Sci. USA* 86, 7522–7526.
19. Weiser, W. Y., Ordonez, D. K., Remold, H. G. & David, J. R. (1981) *J. Immunol.* 126, 1958–1962.
20. Honma, M., Nagahama, M., Kim, W.-S., Watanabe, T., Hatanaka, K., Tsunoo, K., Maruyama, K. & Nakayama, K. (1991) *J. Biol. Chem.* 266, 23137–23140.
21. Kozak, M. (1983) *Microbiol. Rev.* 47, 1–45.
22. Lanahan, A., Williams, J. B., Sanders, L. K. & Nathans, D. (1992) *J. Mol. Cell. Biol.* 12, 3919–3929.
23. Rubartelli, A., Cozzolino, F., Talio, M. & Sitia, R. (1990) *EMBO J.* 9, 1503–1510.

Office Action Summary	Application No.	Applicant(s)	
	10/609,346	YU ET AL.	
	Examiner	Art Unit	
	Prema M. Mertz	1646	

-- The MAILING DATE of this communication appears on the cover sheet with the correspondence address --

Period for Reply

A SHORTENED STATUTORY PERIOD FOR REPLY IS SET TO EXPIRE 3 MONTH(S) OR THIRTY (30) DAYS, WHICHEVER IS LONGER, FROM THE MAILING DATE OF THIS COMMUNICATION.

- Extensions of time may be available under the provisions of 37 CFR 1.136(a). In no event, however, may a reply be timely filed after SIX (6) MONTHS from the mailing date of this communication.
- If NO period for reply is specified above, the maximum statutory period will apply and will expire SIX (6) MONTHS from the mailing date of this communication.
- Failure to reply within the set or extended period for reply will, by statute, cause the application to become ABANDONED (35 U.S.C. § 133). Any reply received by the Office later than three months after the mailing date of this communication, even if timely filed, may reduce any earned patent term adjustment. See 37 CFR 1.704(b).

Status

1)☒ Responsive to communication(s) filed on *14 July 2006*.

2a)☐ This action is **FINAL**. 2b)☒ This action is non-final.

3)☐ Since this application is in condition for allowance except for formal matters, prosecution as to the merits is closed in accordance with the practice under *Ex parte Quayle*, 1935 C.D. 11, 453 O.G. 213.

Disposition of Claims

4)☒ Claim(s) *21-23,27-33,40 and 41* is/are pending in the application.

4a) Of the above claim(s) _____ is/are withdrawn from consideration.

5)☐ Claim(s) _____ is/are allowed.

6)☒ Claim(s) *21-23, 27-33, 40-41* is/are rejected.

7)☐ Claim(s) _____ is/are objected to.

8)☐ Claim(s) _____ are subject to restriction and/or election requirement.

Application Papers

9)☐ The specification is objected to by the Examiner.

10)☐ The drawing(s) filed on _____ is/are: a)☐ accepted or b)☐ objected to by the Examiner.

Applicant may not request that any objection to the drawing(s) be held in abeyance. See 37 CFR 1.85(a).

Replacement drawing sheet(s) including the correction is required if the drawing(s) is objected to. See 37 CFR 1.121(d).

11)☐ The oath or declaration is objected to by the Examiner. Note the attached Office Action or form PTO-152.

Priority under 35 U.S.C. § 119

12)☐ Acknowledgment is made of a claim for foreign priority under 35 U.S.C. § 119(a)-(d) or (f).

a)☐ All b)☐ Some * c)☐ None of:

1.☐ Certified copies of the priority documents have been received.

2.☐ Certified copies of the priority documents have been received in Application No. _____.

3.☐ Copies of the certified copies of the priority documents have been received in this National Stage application from the International Bureau (PCT Rule 17.2(a)).

* See the attached detailed Office action for a list of the certified copies not received.

Attachment(s)

1) ☒ Notice of References Cited (PTO-892)
2) ☐ Notice of Draftsperson's Patent Drawing Review (PTO-948)
3) ☐ Information Disclosure Statement(s) (PTO-1449 or PTO/SB/08) Paper No(s)/Mail Date _____.
4) ☐ Interview Summary (PTO-413) Paper No(s)/Mail Date. _____.
5) ☐ Notice of Informal Patent Application (PTO-152)
6) ☐ Other: _____.

DETAILED ACTION

Election/Restrictions

1. Applicant's election without traverse of Group II (claims 21-23, 27-33, 40-41) in the reply filed on 7/14/2006 is acknowledged. Claims 1-11, 15-20, 24-26, 34-39, 42-50 have been canceled (6/16/2006) and claims 12-14 have been canceled (7/14/2006).

Claims 21-23, 27-33, 40-41, are pending and under consideration by the Examiner.

Claim rejections-35 USC § 112, first paragraph

2. The following is a quotation of the first paragraph of 35 U.S.C. 112:

> The specification shall contain a written description of the invention, and of the manner and process of making and using it, in such full, clear, concise, and exact terms as to enable any person skilled in the art to which it pertains, or with which it is most nearly connected, to make and use the same and shall set forth the best mode contemplated by the inventor of carrying out his invention.

2a. Claims 21-23, 27-33, 40-41, are rejected under 35 U.S.C. 1 12, first paragraph, as failing to comply with the written description requirement. The claims contain subject matter, which was not described in the specification in such a way as to reasonably convey to one skilled in the relevant art that the inventors, at the time the application was filed, had possession of the claimed invention.

The claims are drawn to an isolated nucleic acid having at least 90%, and 95% nucleotide sequence identity with a particular disclosed sequence (SEQ ID NO:7). The claims do not require that the polynucleotide encoding the polypeptide possess any particular conserved structure, or other disclosed distinguishing feature. Thus, the claims are drawn to a genus of polynucleotides encoding polypeptides that is defined only by sequence identity. To provide evidence of possession of a claimed genus, the specification must provide sufficient distinguishing identifying characteristics of the genus. The factors to be considered include

disclosure of complete or partial structure, physical and/or chemical properties, functional characteristics, structure/function correlation, methods of making the claimed product, or any combination thereof. In this case, the only factor present in the claim is a partial structure in the form of a recitation of percent identity. There is not even identification of any particular portion of the structure that must be conserved for the biological activity of the protein. Accordingly, in the absence of sufficient recitation of distinguishing identifying characteristics and structure/function relationship, the specification does not provide adequate written description of the claimed genus.

Vas-cath Inc. v. Mahurkar, 19 USPQ2d 1111, clearly states that "applicant must convey with reasonable clarity to those skilled in the ad that, as of the filing date sought, he or she was in possession *of the invention*. The invention is, for purposes of the written description' inquiry, whatever is *now claimed*." (See page 1117.) The specification does not "clearly allow persons of ordinary skill in the art to recognize that (he or she) invented what is claimed." (See *Vas-Cath* at page 1116). As discussed above, the skilled artisan cannot envision the detailed chemical structure of the encompassed genus of polynucleotides, and therefore conception is not achieved until reduction to practice has occurred, regardless of the complexity or simplicity of the method of isolation. Adequate written description requires more than a mere statement that it is part of the invention and reference to a potential method of isolating it. The compound itself is required. See *Fiers v. Revel*, 25 USPQ2d 1601 at 1606 (CAFC 1993) and *Amgen Inc. v. Chugai Pharmaceutical Co. Ltd.*, 18 USPQ2d 1016.

One cannot describe what one has not conceived. See *Fiddes v. Baird*, 30 USPQ2d 1481 at 1483. In *Fiddes*, claims directed to mammalian FGF'S were found to be unpatentable due to

lack of written description for that broad class. The specification provided only the bovine sequence. Therefore, only a nucleic acid encoding a polypeptide of amino acid sequence set forth in SEQ ID NO:8 as recited in claim 23, but not the full breadth of the claims meets the written description provision of 35 U.S.C. 112, first paragraph. Applicant is reminded that *Vas-Cath* makes clear that the written description provision of 35 U.S.C. 112 is severable from its enablement provision (see page 1115).

2b. Claims 21-23, 27-33, 40-41, are rejected under 35 U.S.C. 112, first paragraph, because the specification, while being enabling for an isolated polynucleotide encoding a polypeptide of amino acid sequence set forth in SEQ ID NO:8, does not reasonably provide enablement for an isolated nucleic acid having at least 90%, and 95% nucleotide sequence identity with a particular disclosed sequence (SEQ ID NO:7). The specification does not enable any person skilled in the art to which it pertains, or with which it is most nearly connected, to make the invention commensurate in scope with these claims.

Claim 21, for example, is overly broad in its limitation of "at least 90% sequence identity" because no guidance is provided as to which of the myriad of nucleic acid molecules encompassed by the claims will encode a polypeptide which retains the characteristics of the desired polypeptide. Variants of a nucleic acid can be generated by deletions, insertions, and substitutions of nucleotides, but no actual or prophetic examples on expected performance parameters of any of the possible variants of the claimed nucleic acid molecule or muteins of the protein molecule have been disclosed. Furthermore, it is known in the art that even single amino acid changes or differences in the amino acid sequence of a protein can have dramatic effects on the protein's function. For example, Mikayama et al. (1993) teaches that the human

glycosylation-inhibiting factor (GIF) protein differs from human migration inhibitory factor (MIF) by a single amino acid residue (page 10056, Figure 1). Yet, despite the fact that these proteins are 90% identical at the amino acid level, GIF is unable to carry out the function of MIF, and MIF does not exhibit GIF bioactivity (page 10059, second column, third paragraph). It is also known in the art that a single amino acid change in a protein's sequence can drastically affect the structure of the protein and the architecture of an entire cell. Voet et al. (1990) teaches that a single Glu to Val substitution in the beta subunit of hemoglobin causes the hemoglobin molecules to associate with one another in such a manner that, in homozygous individuals, erythrocytes are altered from their normal discoid shape and assume the sickle shape characteristic of sickle-cell anemia, causing hemolytic anemia and blood flow blockages (pages 126-128, section 6-3A and page 230, column 2, first paragraph).

There is no guidance provided in the instant specification as to how one of skill in the art would generate and use a nucleic acid having at least 90%, and 95% nucleotide sequence identity with SEQ ID NO:7 other than the polynucleotide of SEQ ID NO:7 exemplified in the specification. See *In re Wands*, 858 F.2d at 737, 8 USPQ2d at 1404. The test of enablement is not whether any experimentation is necessary, but whether, if experimentation is necessary, it is undue. The factors to be considered when determining whether there is sufficient evidence to support a determination that a disclosure does not satisfy the enablement requirement and whether any necessary experimentation is "undue" include, but are not limited to: (1) the breadth of the claims; (2) the nature of the invention; (3) the state of the prior art; (4) the level of one of ordinary skill; (5) the level of predictability in the art; (6) the amount of direction provided by

the inventor; (7) the existence of working examples; and (8) the quantity of experimentation needed to make or use the invention based on the content of the disclosure.

Given the breadth of the claims, in light of the predictability of the art as determined by the number of working examples, the level of skill of the artisan, and the guidance provided in the instant specification and the prior art of record, it would require undue experimentation for one of ordinary skill in the art to make and use the claimed invention.

Claim Rejections - 35 USC § 112, second paragraph

3. The following is a quotation of the second paragraph of 35 U.S.C. 112:

> The specification shall conclude with one or more claims particularly pointing out and distinctly claiming the subject matter which the applicant regards as his invention.

Claims 21-23, 27-33, 40-41 are rejected under 35 U.S.C. 112, second paragraph, as being indefinite for failing to particularly point out and distinctly claim the subject matter which applicant regards as the invention.

Claim 21, is vague and indefinite because it recites "comprising: a nucleotide sequence at least...." rather than "comprising a nucleotide sequence....".

Claim 27, line 2, is vague and indefinite because it recites "specific antibody of human albumin". It is unclear what this term means.

Claim 28, is vague and indefinite because it recites "comprising: the sequence of the polynucleotide...." rather than "comprising the polynucleotide ....".

Claim 31 is vague and indefinite because it recites "but not limited, Saccharomyces...." rather than "but not limited to Saccharomyces....".

Claim 32 is vague and indefinite because it is incomplete. Furthermore, the claim if complete would be a duplicate of claim 31. It is suggested that this claim be deleted.

Claims 22-23, 29-30, 33, 40-41 are rejected as vague and indefinite insofar as they depend on the above rejected claims for their limitations.

Claim Rejections - 35 USC § 103

4. The following is a quotation of 35 U.S.C. 103(a) which forms the basis for all obviousness rejections set forth in this Office action:

(a) A patent may not be obtained though the invention is not identically disclosed or described as set forth in section 102 of this title, if the differences between the subject matter sought to be patented and the prior art are such that the subject matter as a whole would have been obvious at the time the invention was made to a person having ordinary skill in the art to which said subject matter pertains. Patentability shall not be negatived by the manner in which the invention was made.

The factual inquiries set forth in Graham v. John Deere Co., 383 U.S. 1, 148 USPQ 459 (1966), that are applied for establishing a background for determining obviousness under 35 U.S.C. 103(a) are summarized as follows:

1. Determining the scope and contents of the prior art.
2. Ascertaining the differences between the prior art and the claims at issue.
3. Resolving the level of ordinary skill in the pertinent art.
4. Considering objective evidence present in the application indicating obviousness or nonobviousness.

Claims 21-23, 27-33, 40-41 are rejected under 35 U.S.C. 103(a) as being unpatentable over Shaw (4,904,584) in view of the Capon et al. patent (U.S. Patent No. 5,116,964).

The Shaw patent discloses a polynucleotide encoding a human G-CSF protein, vectors for recombinant vectors for expression of the protein and host cells for producing the recombinant protein (see abstract; column 1, lines 5-14; columns 10-12, Examples 1, 2 and 3). A comparison of the amino acid sequence presented in Figure 4 of the Shaw patent with the amino

acid sequence of G-SCF presented in Figure 1(H) of the instant application supports the conclusion that the G-CSF protein of Shaw patent is the same as the G-CSF polypeptide of the instant invention. However, Shaw does not disclose a polynucleotide encoding both G-CSF and albumin to obtain a fusion protein comprising albumin and G-CSF to increase the half-life of the G-CSF.

Capon et al. teaches chimeric proteins for directing ligand binding partners such as growth factors, hormones or effector molecules to cells bearing ligands for the ligand binding partners comprising a ligand binding partner fused to a stable plasma protein which is capable of extending the in vivo half-life of the ligand binding partner when present as a fusion with the ligand binding partner, in particular wherein such a stable plasma protein is an immunoglobulin constant domain or albumin (see column 4, lines 57-64; column 5, lines 11-21; column 7, lines 11-27; column 8, lines 13-15).

Therefore, it would have been prima facie obvious to one having ordinary skill in the art to modify the polynucleotide of Shaw such that it includes both, the polynucleotide encoding G-CSF and the polynucleotide encoding albumin, to obtain a chimeric protein with an increased circulating half-life, as taught by Capon et al., to obtain the known functions and advantages of the G-CSF polypeptide as per the teachings of Shaw. Cytokines such as G-CSF are well-known in the art as having a short half-life. One would have been motivated to use a chimeric polynucleotide encoding a chimeric protein comprising G-CSF and albumin to decrease the clearance rate of G-CSF *in vivo*. Therefore, it would have been obvious to obtain a chimeric polynucleotide encoding G-CSF and albumin, a long-lived molecule well known in the art as able to increase the stability of rapidly cleared molecules.

Conclusion

No claim is allowed.

Claims 21-23, 27-33, 40-41, are rejected.

Advisory Information

Any inquiry concerning this communication or earlier communications from the examiner should be directed to Prema Mertz whose telephone number is (571) 272-0876. The examiner can normally be reached on Monday-Friday from 7:00AM to 3:30PM (Eastern time).

If attempts to reach the examiner by telephone are unsuccessful, the examiner's supervisor, Gary Nickol, can be reached on (571) 272-0835.

Official papers filed by fax should be directed to (571) 273-8300. Faxed draft or informal communications with the examiner should be directed to (571) 273-0876.

Information regarding the status of an application may be obtained from the Patent application Information Retrieval (PAIR) system. Status information for published applications may be obtained from either Private PAIR or Public PAIR. Status information for unpublished applications is available through Private PAIR only. For more information about the PAIR system, see http://pair-direct.uspto.gov. Should you have questions on access to the Private PAIR system, contact the Electronic Business Center (EBC) at 866-217-9197 (toll-free).

Prema Mertz

Prema Mertz Ph.D., J.D.
Primary Examiner
Art Unit 1646
August 18, 2006

Notice of References Cited	Application/Control No. 10/609,346	Applicant(s)/Patent Under Reexamination YU ET AL.	
	Examiner Prema M. Mertz	Art Unit 1646	Page 1 of 1

U.S. PATENT DOCUMENTS

*		Document Number Country Code-Number-Kind Code	Date MM-YYYY	Name	Classification
*	A	US-4,904,584	02-1990	Shaw, Gray	435/69.4
*	B	US-5,116,964	05-1992	Capon et al.	536/23.5
	C	US-			
	D	US-			
	E	US-			
	F	US-			
	G	US-			
	H	US-			
	I	US-			
	J	US-			
	K	US-			
	L	US-			
	M	US-			

FOREIGN PATENT DOCUMENTS

*		Document Number Country Code-Number-Kind Code	Date MM-YYYY	Country	Name	Classification
	N					
	O					
	P					
	Q					
	R					
	S					
	T					

NON-PATENT DOCUMENTS

*		Include as applicable: Author, Title Date, Publisher, Edition or Volume, Pertinent Pages)
	U	Mikayama et al. Proc. Natl. Acad. Sci. USA Vol. 90, pages 10056-10060.
	V	Voet et al. Biochemistry John Wiley & Sons, Inc., pages 126-128 and 228-234.
	W	
	X	

*A copy of this reference is not being furnished with this Office action. (See MPEP § 707.05(a).)
Dates in MM-YYYY format are publication dates. Classifications may be US or foreign.